EXCITONS, PLASMONS, AND EXCITONIC COMPLEXES IN QUASI-1D SEMICONDUCTORS. THEORETICAL PERSPECTIVE

Igor Bondarev

Math & Physics Department
North Carolina Central University
Durham, NC 27707, USA

Lilia Woods group

W.Domcke group, TU Munich

US National Science Foundation – ECCS-1306871
US Department of Energy – DE-SC0007117

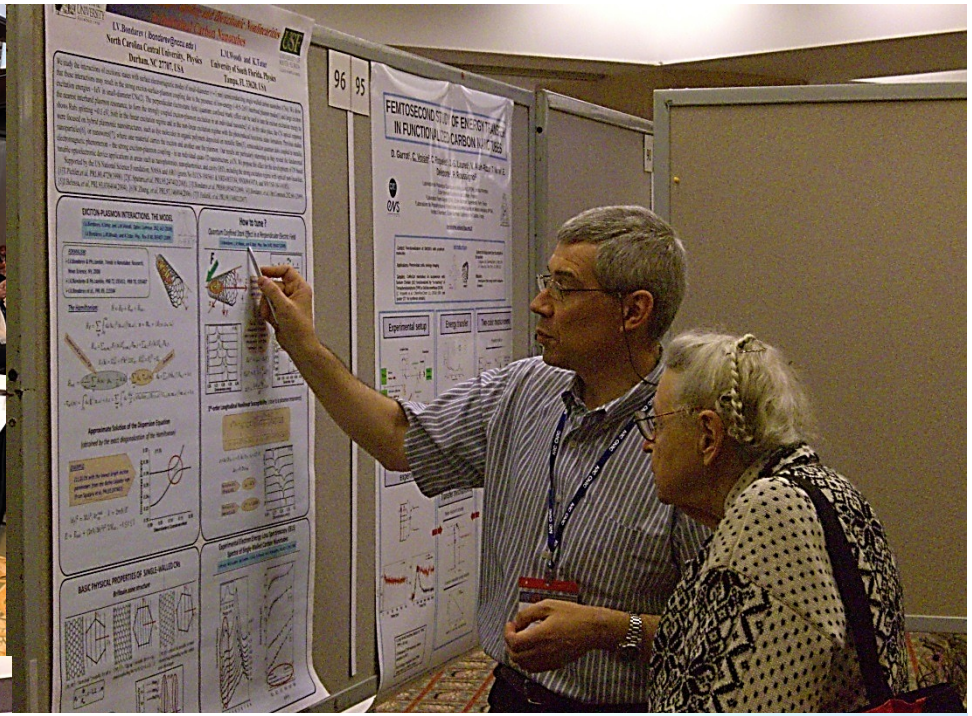
96
95


96
95

OUTLINE

- ***Pristine Semiconducting Carbon Nanotubes:***
  Excitons and Interband Plasmons – Brief Review

- ***Plasmon Generation by Optically Excited Excitons, Exciton BEC Effect***

- ***Excitonic Complexes (Biexcitons & Trions) in quasi-1D:***
  Brief Review, Landau-Herring Approach to Understand Relative Stability

- ***Hybrid Carbon Nanotube Systems:*** ***Plasmon Enhanced Raman Scattering Effect, Transmission Fano Resonances in Hybrid Metal-Encapsulating Semiconducting CNs, CN arrays***

- ***Summary***

CARBON ALLOTROPES

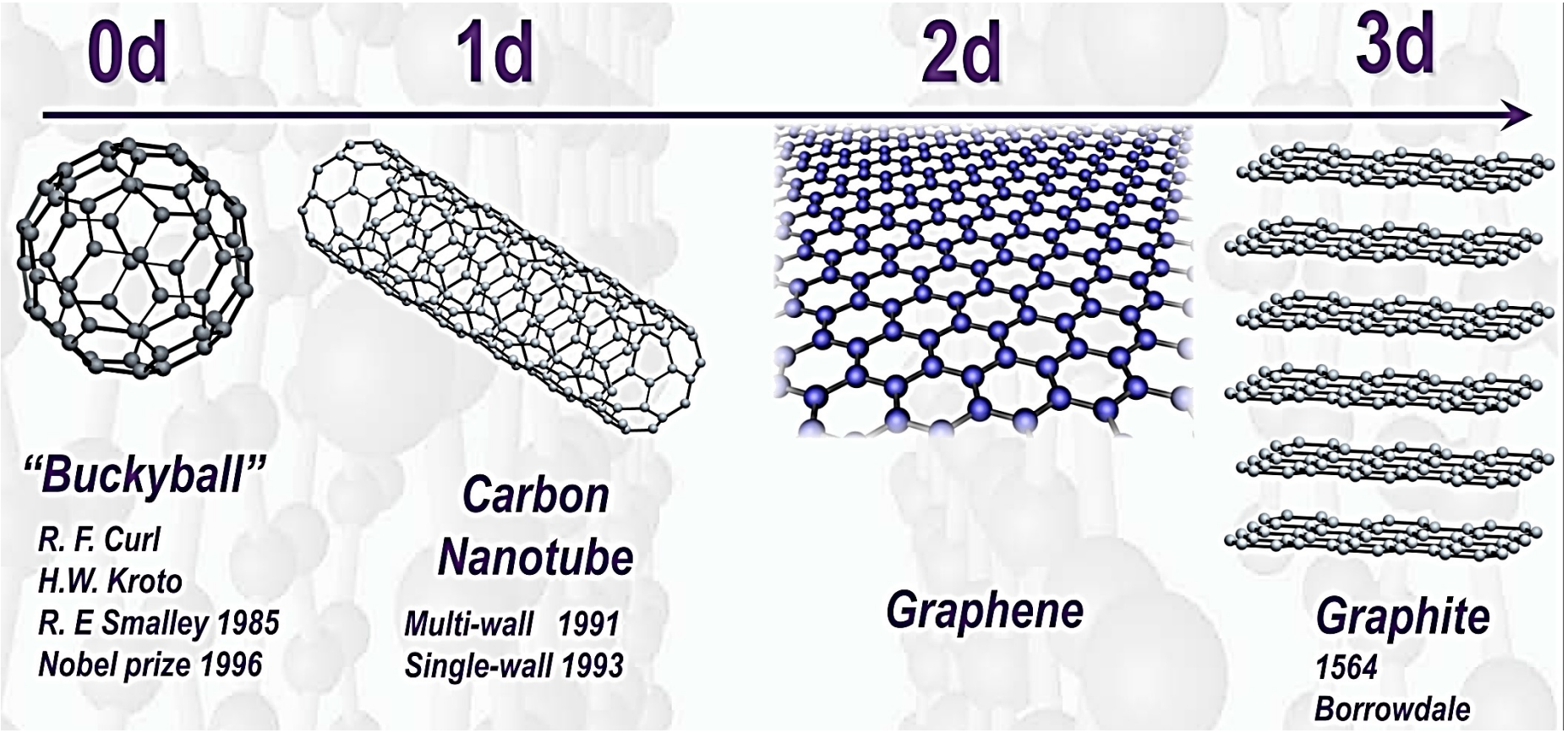

ARTICLES
PUBLISHED ONLINE: 18 APRIL 2016 | DOI: 10.1038/NPHOTON.2016.70
nature photonics

Cavity-enhanced light emission from electrically driven carbon nanotubes

Felix Pyatkov[1,2†], Valentin Fütterling[1†], Svetlana Khasminskaya[1], Benjamin S. Flavel[1], Frank Hennrich[1], Manfred M. Kappes[1,3], Ralph Krupke[1,2*] and Wolfram H. P. Pernice[1,4*]

nature COMMUNICATIONS
Received 9 Jun 2016 | Accepted 1 Sep 2016 | Published 10 Oct 2016 DOI: 10.1038/ncomms13078

Near-infrared exciton-polaritons in strongly coupled single-walled carbon nanotube microcavities

Arko Graf[1,2], Laura Tropf[2], Yuriy Zakharko[1], Jana Zaumseil[1] & Malte C. Gather[2]

LETTERS
PUBLISHED ONLINE: 2 FEBRUARY 2015 | DOI: 10.1038/NNANO.2015.1
nature nanotechnology

Asymmetric dyes align inside carbon nanotubes to yield a large nonlinear optical response

Sofie Cambré[1†], Jochen Campo[1†], Charlie Beirnaert[1], Christof Verlackt[1], Pegie Cool[2] and Wim Wenseleers[1*]

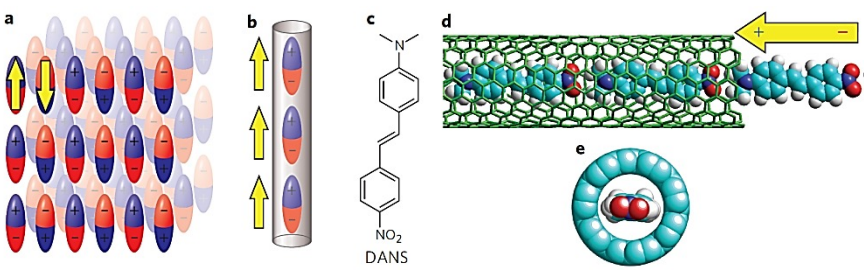

nature nanotechnology
LETTERS
PUBLISHED ONLINE: 13 JULY 2015 | DOI: 10.1038/NNANO.2015.136

Room-temperature single-photon generation from solitary dopants of carbon nanotubes

Xuedan Ma, Nicolai F. Hartmann, Jon K. S. Baldwin, Stephen K. Doorn* and Han Htoon*

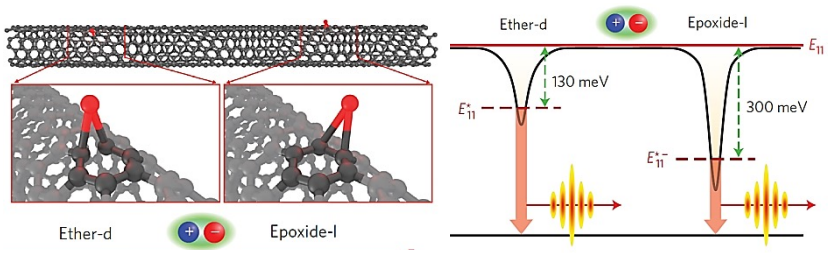

nature nanotechnology
LETTERS
PUBLISHED ONLINE: 28 SEPTEMBER 2015 | DOI: 10.1038/NNANO.2015.220

A carbon nanotube optical rectenna

Asha Sharma[1,2†], Virendra Singh[1†], Thomas L. Bougher[1†] and Baratunde A. Cola[1,3*]

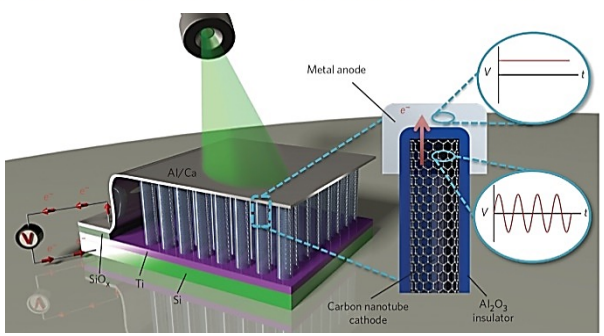

nature nanotechnology
ARTICLES
PUBLISHED ONLINE: 4 APRIL 2016 | DOI: 10.1038/NNANO.2016.44

Wafer-scale monodomain films of spontaneously aligned single-walled carbon nanotubes

Xiaowei He[1‡], Weilu Gao[1‡], Lijuan Xie[2], Bo Li[3], Qi Zhang[1], Sidong Lei[3], John M. Robinson[1†], Erik H. Hároz[4], Stephen K. Doorn[4], Weipeng Wang[3], Robert Vajtai[3], Pulickel M. Ajayan[3], W. Wade Adams[3], Robert H. Hauge[3,5] and Junichiro Kono[1,3,6*]

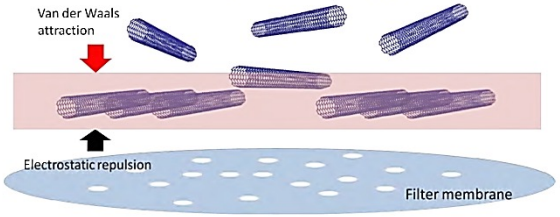

Figure S13. A schematic diagram shows the formation of CNT alignment in a confined region near the surface of the filter membrane.

BASIC PHYSICAL PROPERTIES OF SINGLE-WALLED CARBON NANOTUBES

Classification

Graphene single sheet

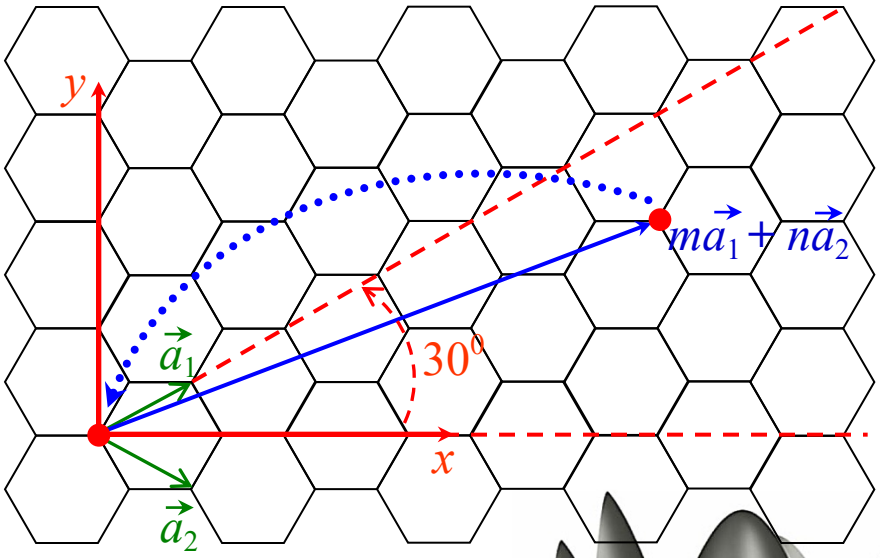

Single-walled CN of (*m*,*n*) type

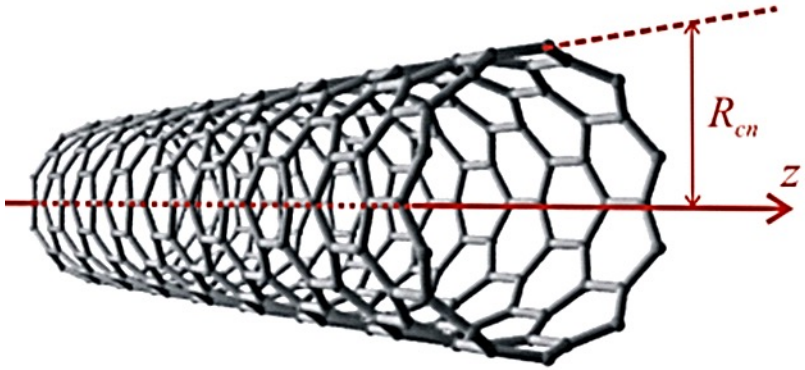

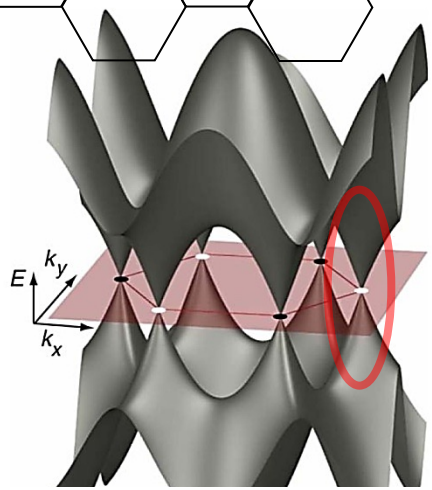

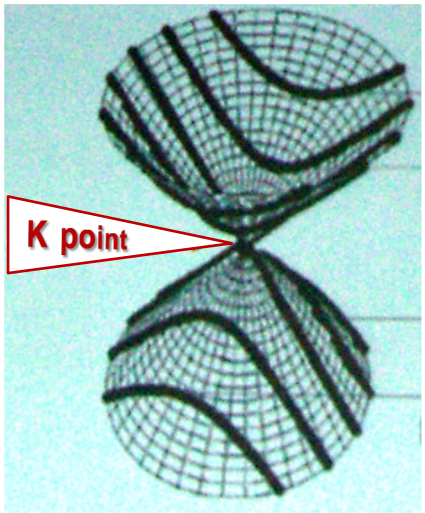

BASIC PHYSICAL PROPERTIES OF SINGLE-WALLED CNs

Brillouin zone structure and longitudinal conductivity

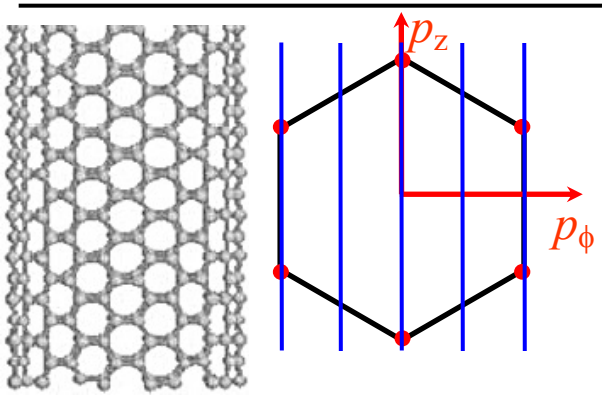

(m,m) – "Armchair": metallic for all m

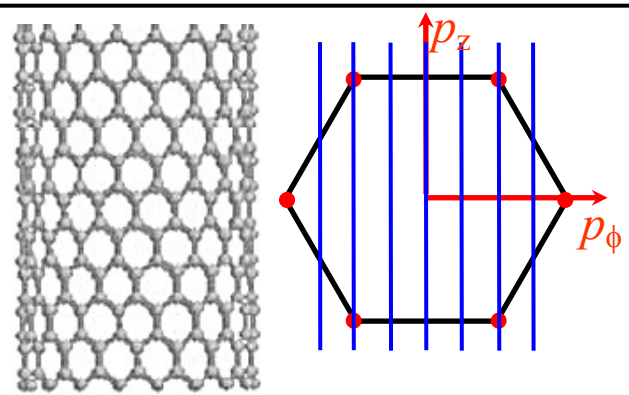

$(m,0)$ – "Zigzag": metallic for $m=3q$, semiconducting for $m\neq 3q$ ($q=1,2,3,\ldots$)

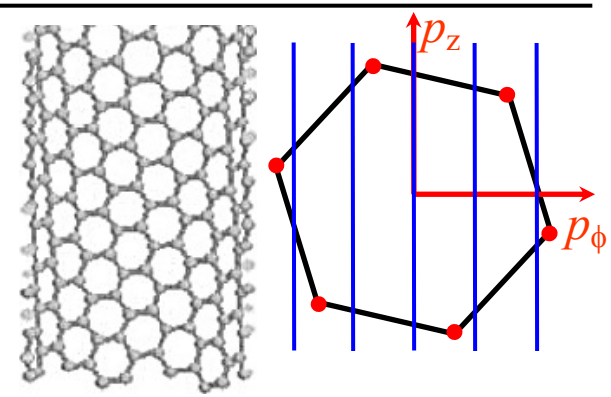

(m,n) – chiral CN: metallic or semi-conducting depending on the radius and chiral angle

$$p_\phi = \frac{\hbar s}{R_{cn}},\ s = 1,2,\ldots,m$$

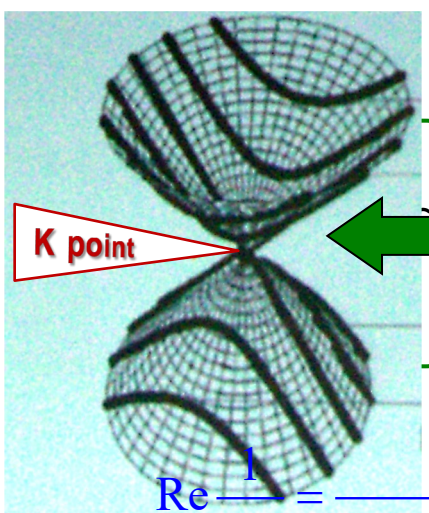

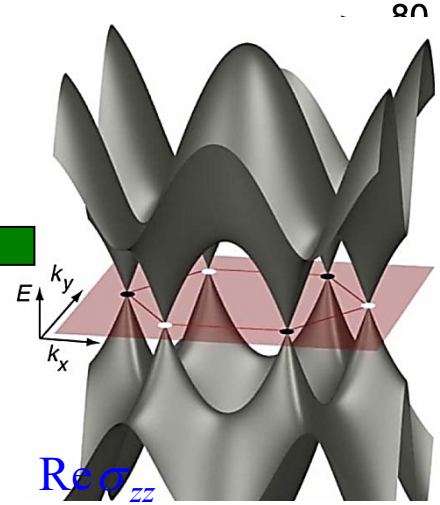

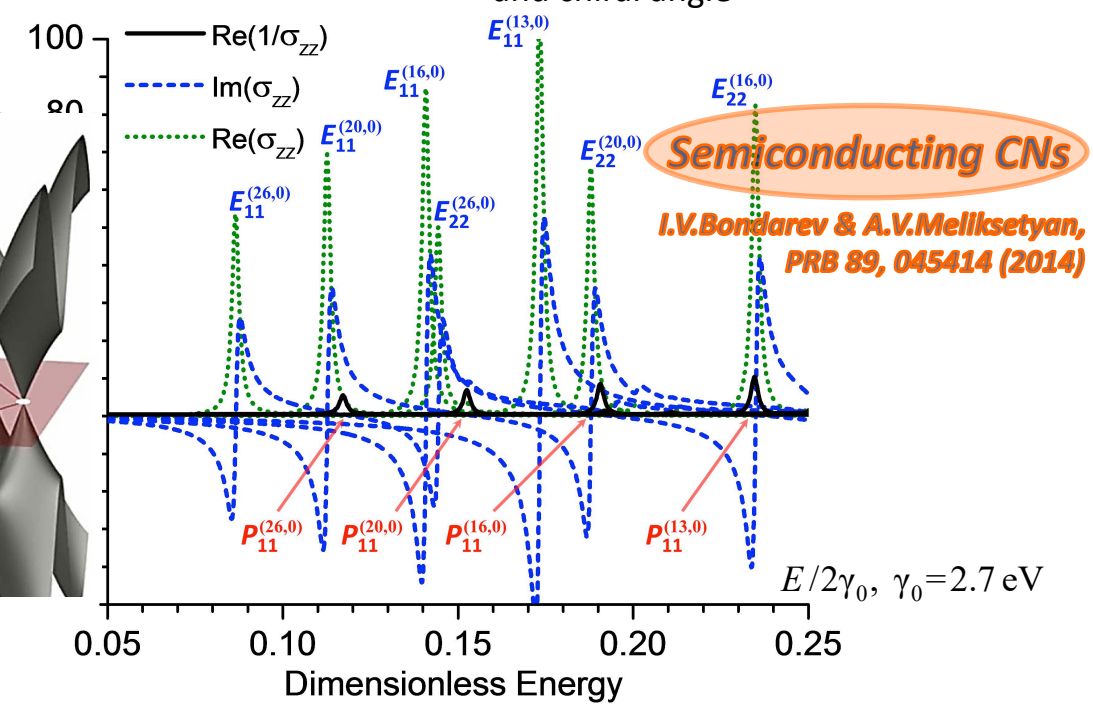

Semiconducting CNs

I.V.Bondarev & A.V.Meliksetyan, PRB 89, 045414 (2014)

$$\mathrm{Re}\frac{1}{\sigma_{zz}} = \frac{\mathrm{Re}\,\sigma_{zz}}{(\mathrm{Re}\,\sigma_{zz})^2 + (\mathrm{Im}\,\sigma_{zz})^2}$$

EXPERIMENTAL ELECTRON ENERGY LOSS SPECTROSCOPY (EELS) SPECTRA OF SINGLE-WALLED CARBON NANOTUBES

T.Pichler, M.Knupher, M.Golden, J.Fink, A.Rinzler, and R.Smalley, PRL 80, 4729 (1998)

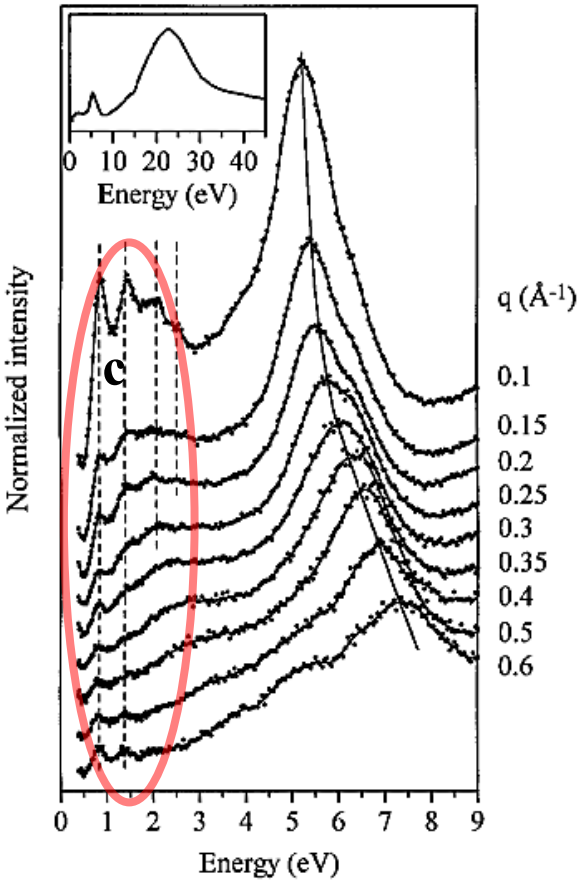

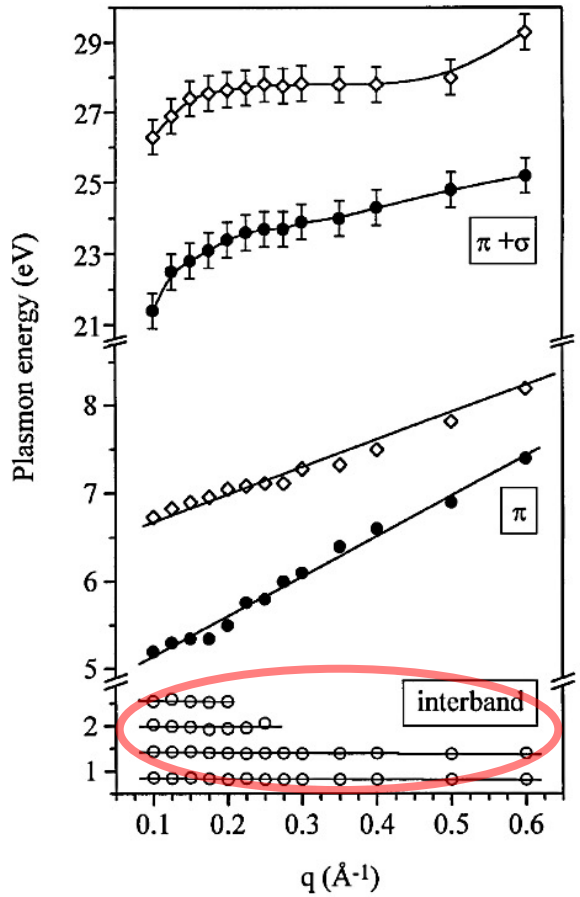

Energy loss function:

$$\sim -\mathrm{Im}\frac{1}{\varepsilon(\omega,q)} \sim \mathrm{Re}\frac{1}{\sigma(\omega,q)}$$

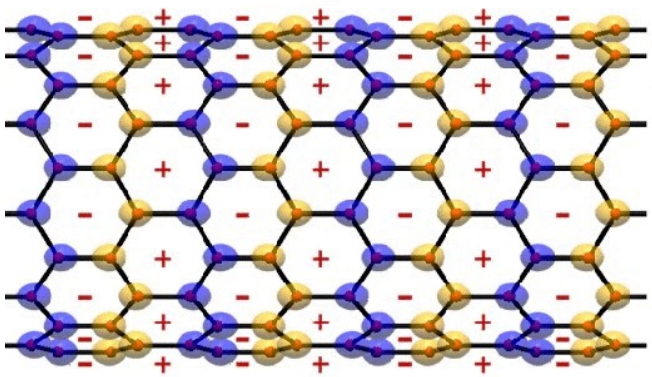

EXCITON AND PLASMON CHARACTERISTICS

$$\mathrm{Re}(1/\sigma_{zz}) = \frac{\mathrm{Re}(\sigma_{zz})}{(\mathrm{Re}(\sigma_{zz}))^2+(\mathrm{Im}(\sigma_{zz}))^2}$$

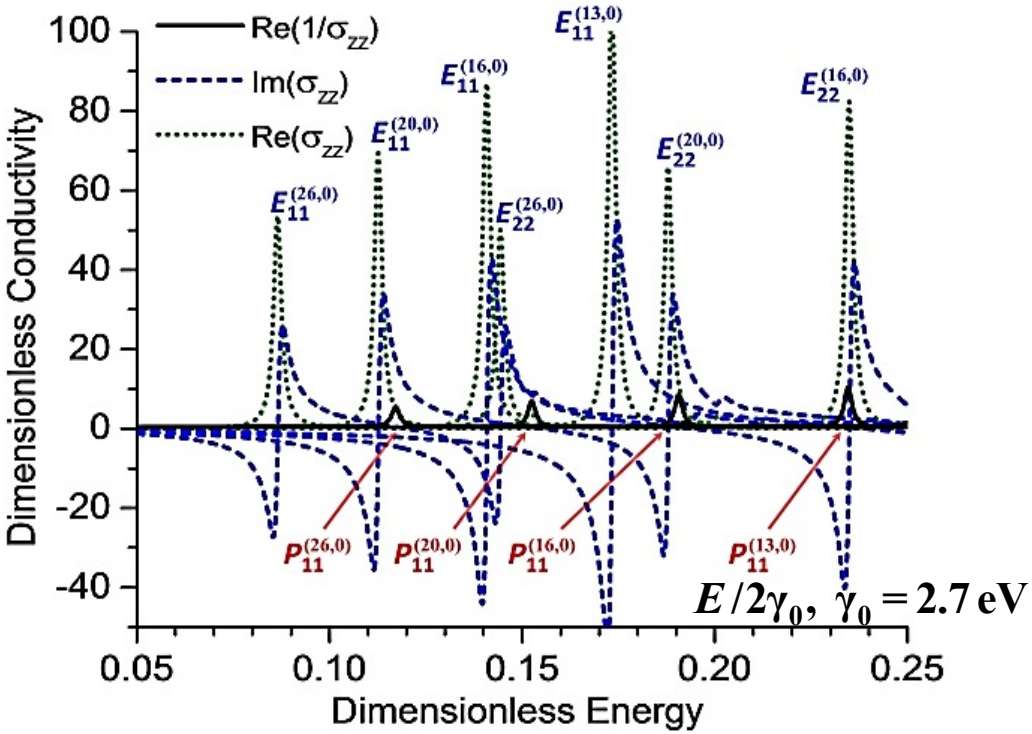

Exciton

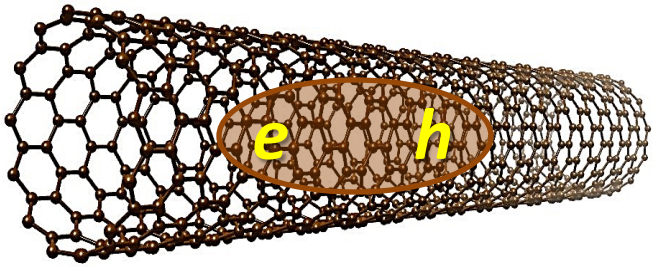

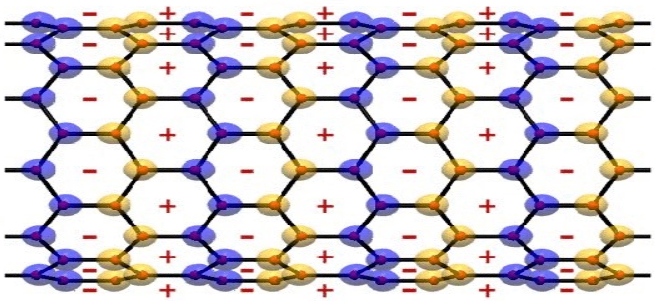

Interband Plasmon *is*
a *standing* charge density wave

- Peak positions are given by CN diameter and chirality
- Excitons and plasmons are in the same energy range – can couple

Atom-Nanotube van der Waals Energy

Role of Interband Plasmons of Individual Nanotubes

I.V.Bondarev & Ph.Lambin, Phys. Rev. B 72, 035451 (2005); Solid State Commun. 132, 203 (2004)

Atom at a fixed distance from the surface inside and outside different zigzag nanotubes of increasing radius

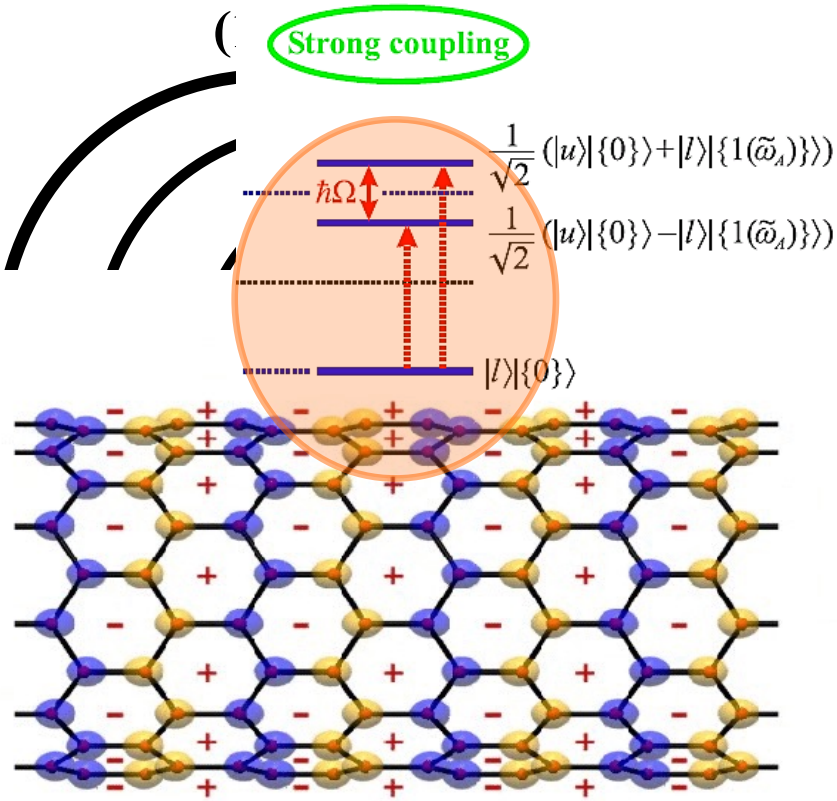

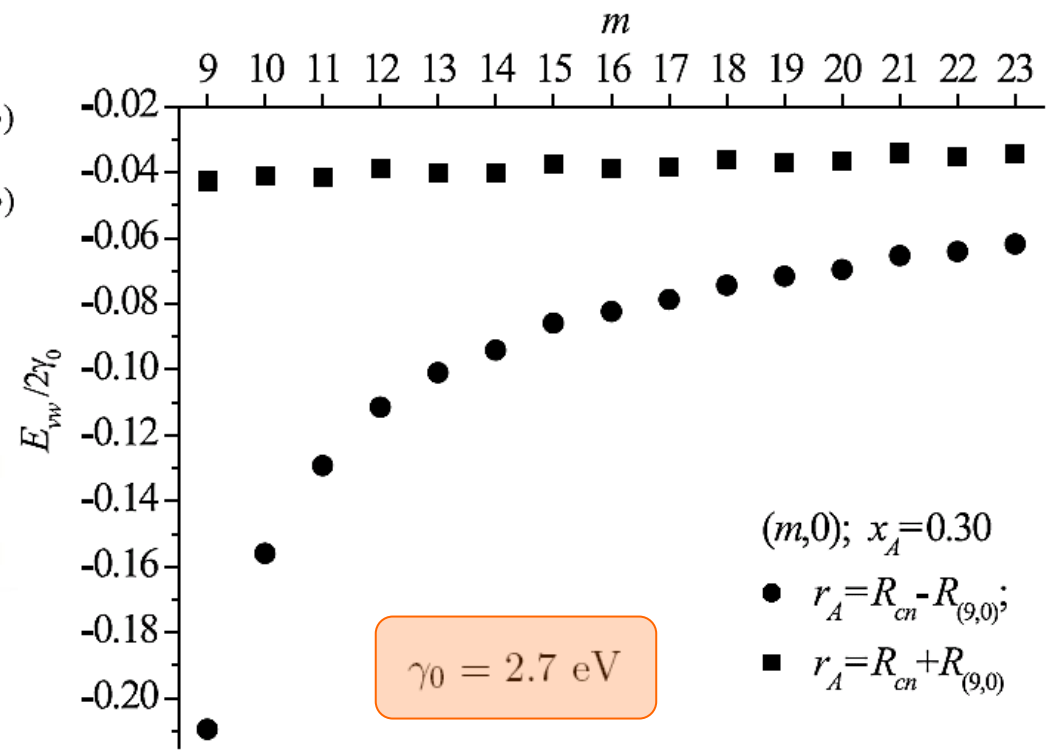

$$d_z E_z^{(loc)}(\mathbf{r}_A) \sim \hbar\Omega$$

Casimir Interaction in Double Wall Carbon Nanotubes

Role of Interband Plasmons of Individual Nanotubes

A.Popescu, L.M.Woods & I.V.Bondarev, Phys. Rev. B 83, 081406(R) (2011)

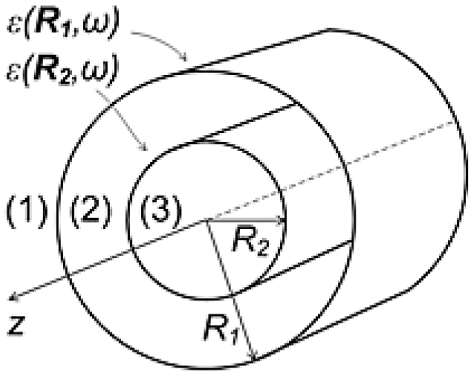

Our calculations explain electron diffraction data by Iijima's group: K.Hirahara et al., Phys. Rev. B 73, 195420 (2006)

$$d = R_1 - R_2$$

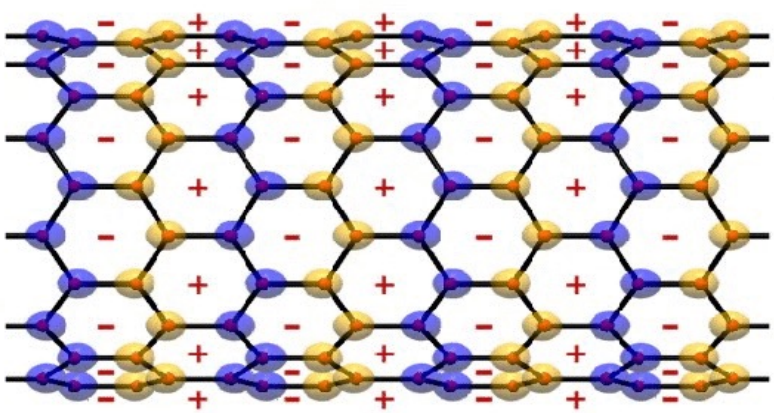

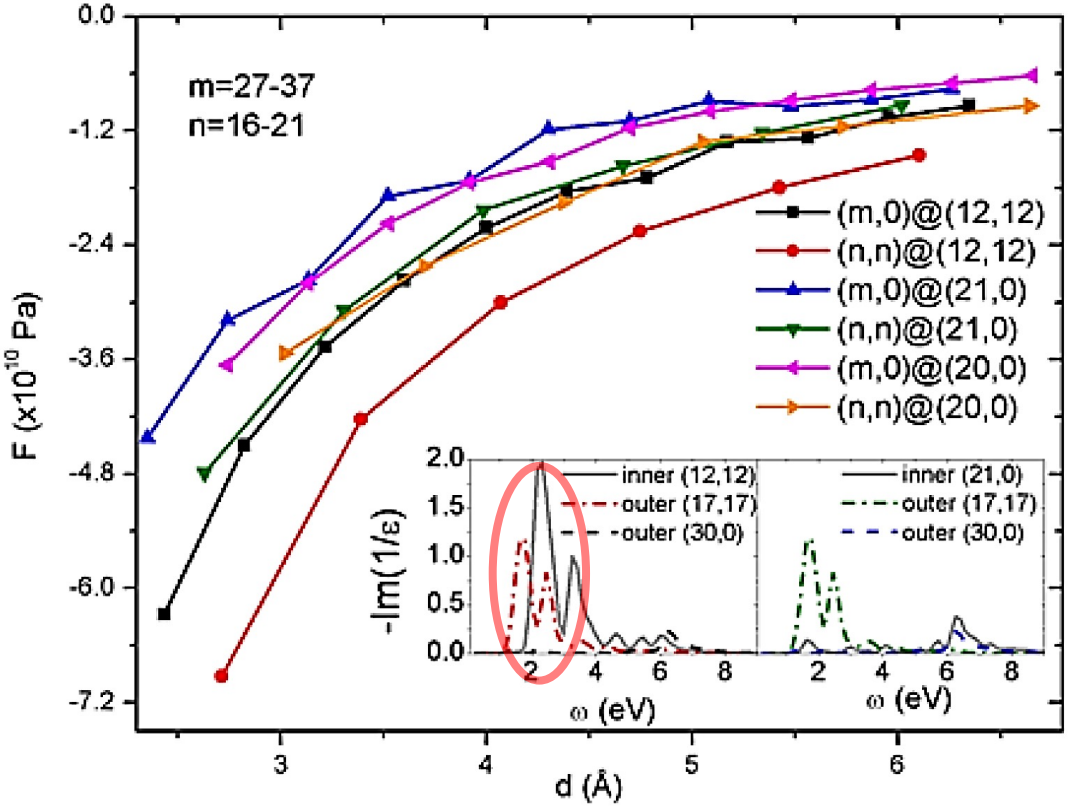

OUTLINE

- ***Pristine Semiconducting Carbon Nanotubes:***
  Excitons and Interband Plasmons – Brief Review

- ***Plasmon Generation by Optically Excited Excitons, Exciton BEC Effect***

- ***Excitonic Complexes (Biexcitons & Trions) in quasi-1D:***
  Brief Review, Understanding Their Relative Stability

- ***Hybrid Carbon Nanotube Systems:*** ***Plasmon Enhanced Raman Scattering Effect, Transmission Fano Resonances in Hybrid Metal-Encapsulating Semiconducting CNs, CN arrays***

- ***Summary***

SOLUTION TO THE DISPERSION EQUATION

(*exact diagonalization of the total Hamiltonian*)

I.V.Bondarev, L.M.Woods and K.Tatur, Phys. Rev. B 80, 085407 (2009)

$$x_{1,2} = \sqrt{\frac{\varepsilon_f^2 + x_p^2}{2} \pm \frac{1}{2}\sqrt{(\varepsilon_f^2 - x_p^2)^2 + (2X_f)^2 \varepsilon_f x_p}}$$

$$\varepsilon_f = E_f(\mathbf{k})/2\gamma_0,\ x_p = E_p/2\gamma_0,\ X_f = [2\Delta x_p \bar{\Gamma}_0^f(x_p)\rho(x_p)]^{1/2},\ \rho(x) \approx \rho(x_p)\Delta x_p^2/[(x-x_p)^2 + \Delta x_p^2]$$

EXAMPLE:

(11,0) ***CN with the lowest bright exciton parameters from the Bethe-Salpeter eqn***
[from Spataru et al, PRL 95, 247402]

$$|d_f|^2 = 3\hbar\lambda^3/4\tau_{ex}^{rad}\ ,\ \lambda = 2\pi c\hbar/E$$

$$E = E_{exc} + (2\pi\hbar/3b)^2 t^2/2M_{ex}\ ,\ -1 \le t \le 1$$

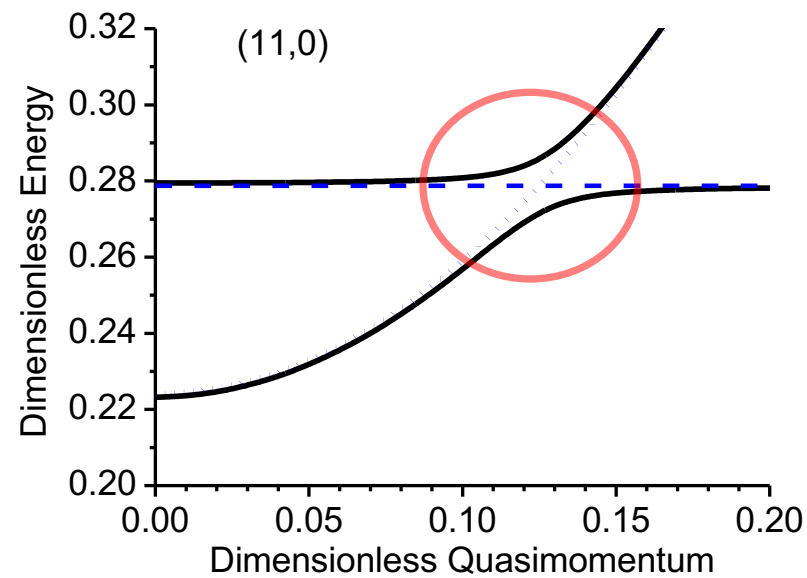

How to couple excitons to interband plasmons ?

Quantum Confined Stark Effect in a Perpendicular Electrostatic Field

I.V.Bondarev, L.M.Woods, and K.Tatur, Phys. Rev. B 80, 085407 (2009)

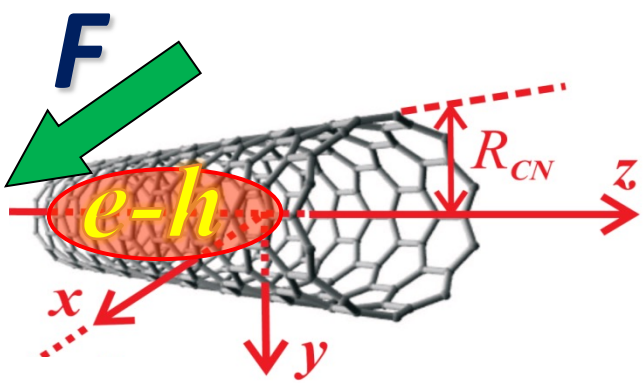

Longitudinal Coulomb potential as field increases

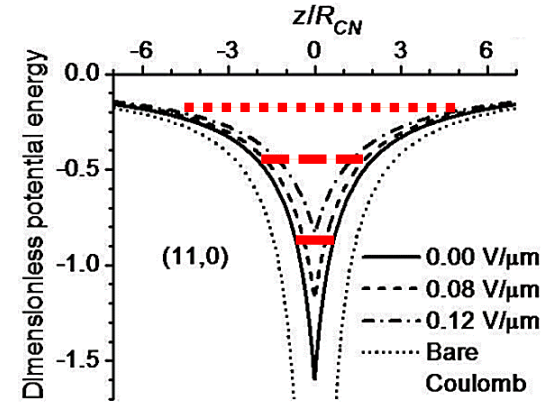

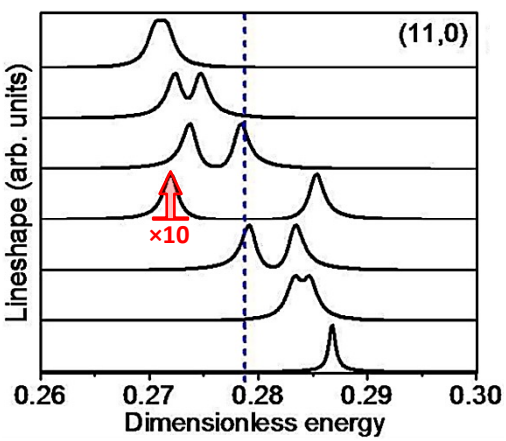

Exciton absorption when tuned to the plasmon resonance

Exciton-plasmon parameters as field increases

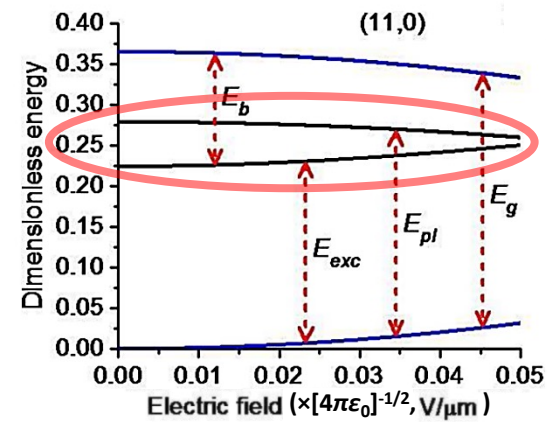

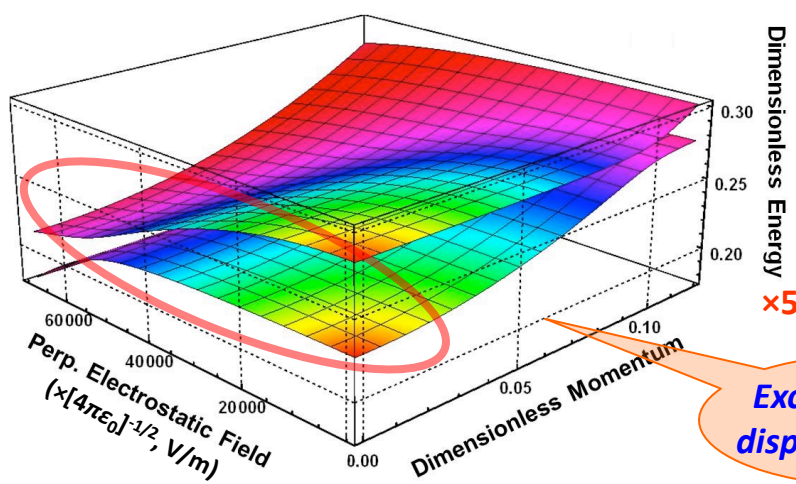

×5.4 eV

Exciton-plasmon dispersion relation

INCREASED ELECTROMAGNETIC ABSORPTION DUE TO PLASMON GENERATION BY OPTICALLY EXCITED EXCITONS

I.V.Bondarev, Phys. Rev. B 85, 035448 (2012)
I.V.Bondarev & T.Antonijevic, Phys. Stat. Sol. C 9, 1259 (2012)

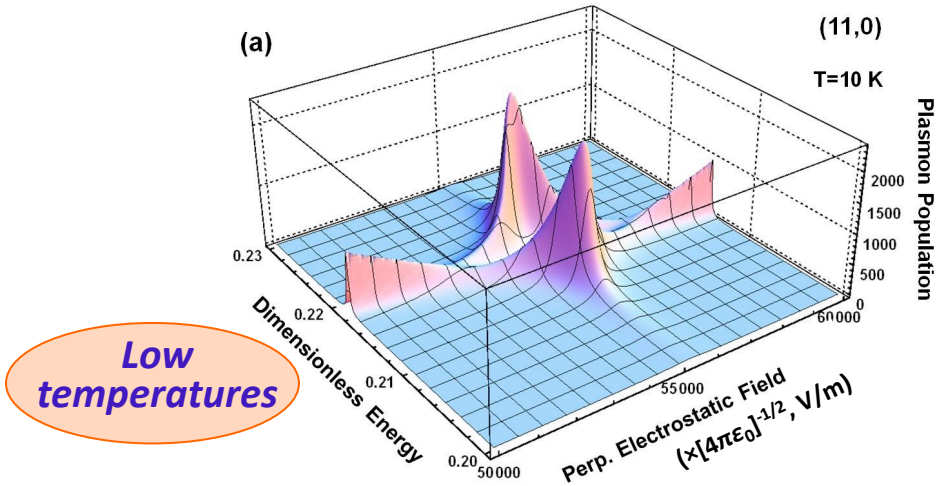

Low temperatures

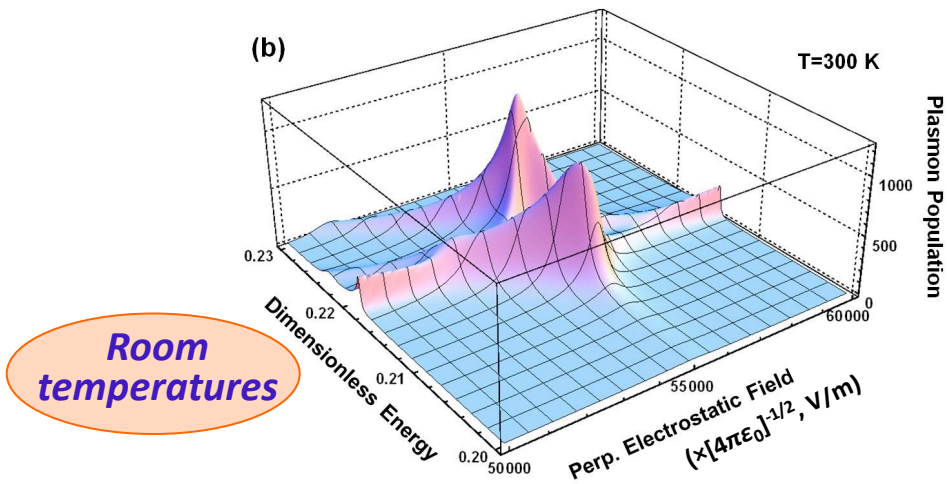

Room temperatures

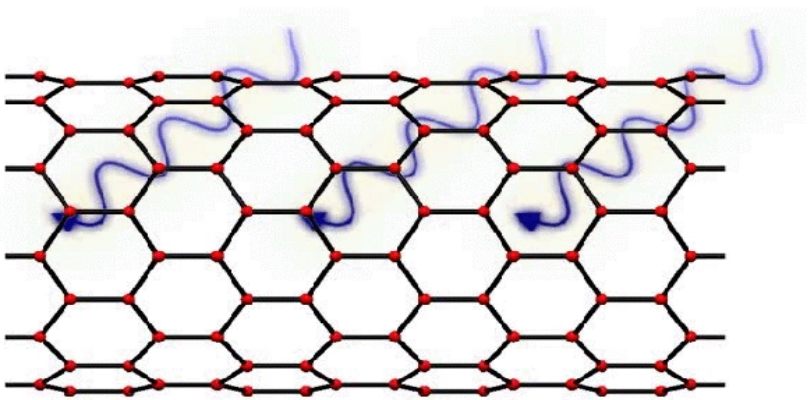

$$E_z = \sqrt{\langle [-\nabla_{\mathbf{n}}\, \hat{\varphi}(\mathbf{n})]_z^2 \rangle}$$

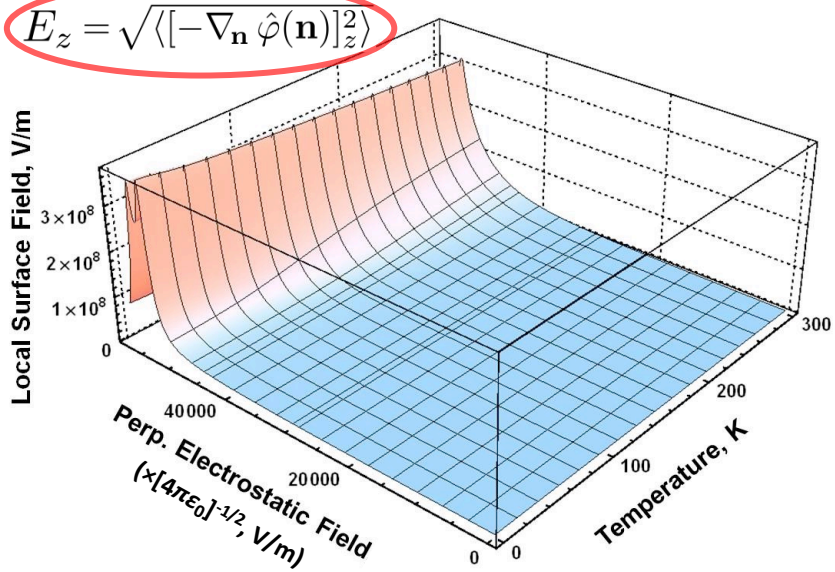

QUANTUM CONFINED STARK EFFECT AND BEC OF EXCITON-PLASMONS IN INDIVIDUAL NANOTUBES

I.V.Bondarev and A.V.Meliksetyan, Phys. Rev. B 89, 045414 (2014)

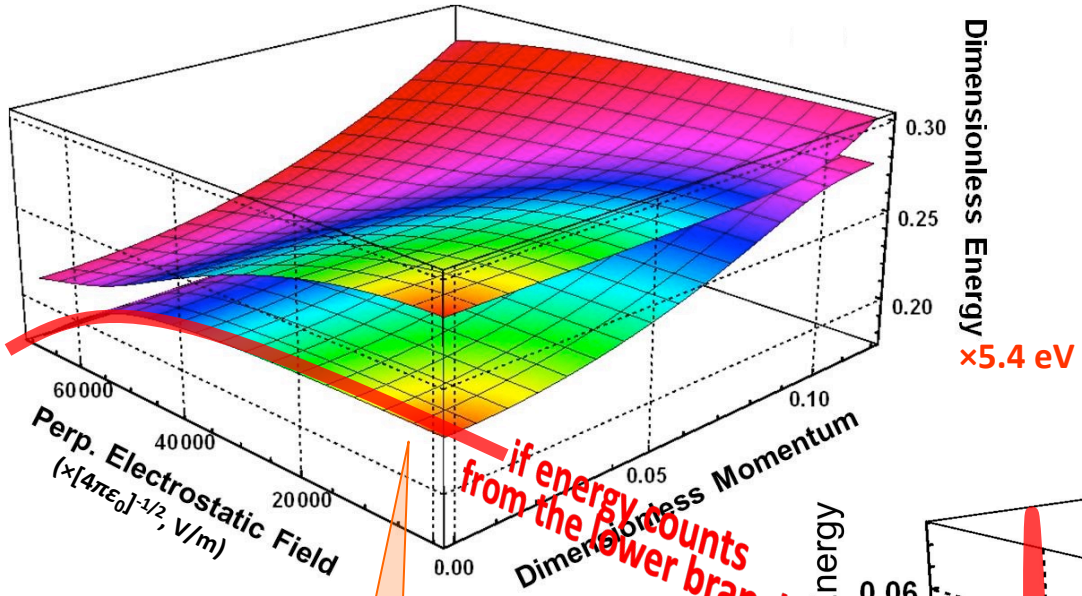

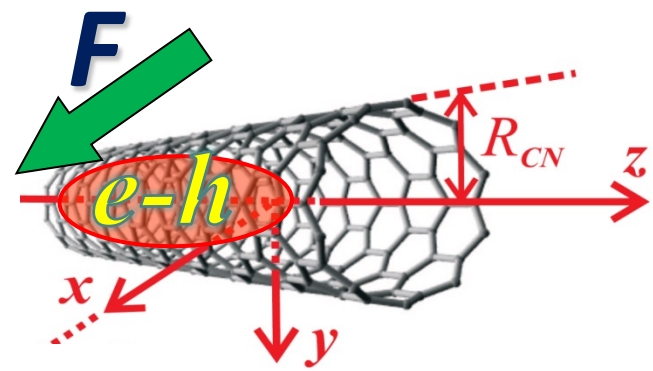

if energy counts from the lower branch

I.V.Bondarev, PRB 85, 035448 (2012)

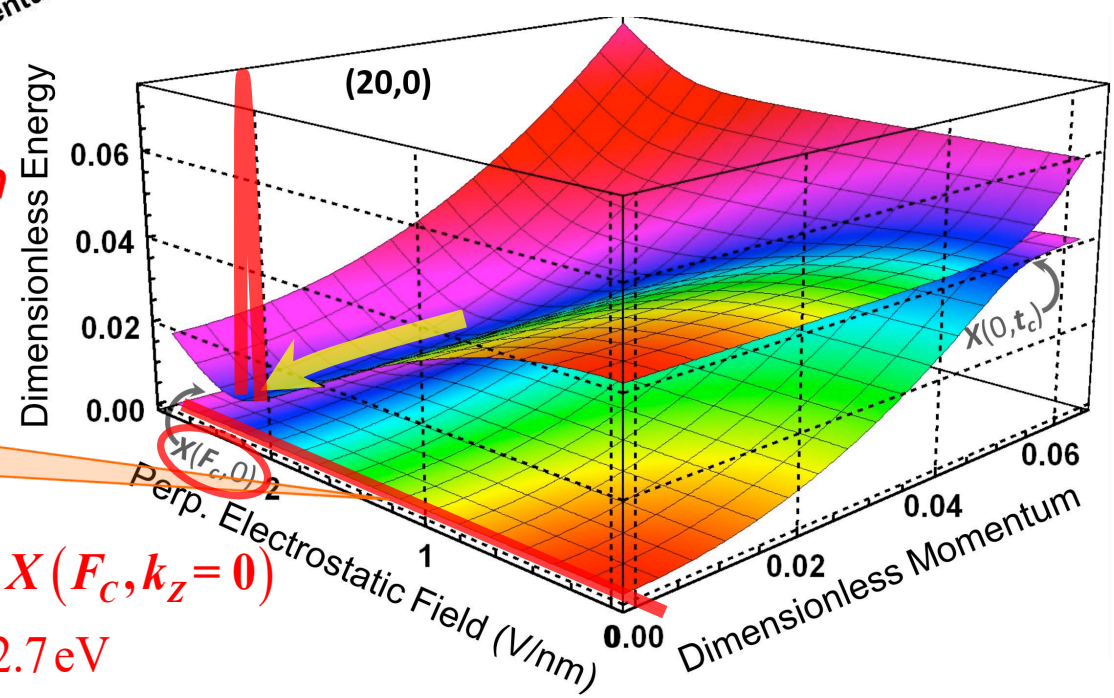

Exciton-plasmon dispersion relation

Exciton-plasmon dispersion relation

$$T < T_C = \left(2\gamma_0/k_B\right) X\left(F_C, k_z = 0\right)$$

$$\gamma_0 = 2.7\,\mathrm{eV}$$

HOW DOES IT COME THAT THIS IS POSSIBLE ??

Here is how… Just basics, nothing else…

(R.Feynman, Statistical Mechanics)

$$g = s\frac{1}{\beta}\int \ln\left(1 - e^{-\beta p^2/2m}e^{\beta\mu}\right)\frac{d^3p}{(2\pi\hbar)^3}V, \qquad \rho = \frac{\langle N\rangle}{V} = -\frac{1}{V}\frac{\partial g}{\partial\mu} = s\int\frac{e^{-\beta p^2/2m}e^{\beta\mu}}{1 - e^{-\beta p^2/2m}e^{\beta\mu}}\frac{d^3p}{(2\pi\hbar)^3}$$

3D 3D

$$dp \xleftarrow{1D} \frac{d^3p}{(2\pi\hbar)^3} \rightarrow \frac{4\pi p^2 dp}{(2\pi\hbar)^3} = \frac{x^2}{2\pi^2\hbar^3}\left(\frac{2m}{\beta}\right)^{3/2}dx, \quad x^2 = \beta p^2/2m \qquad \varepsilon = \frac{p^2}{2m} = \frac{\hbar^2k^2}{2m}$$

$$\rho = s\int_0^\infty \frac{e^{-x^2}\alpha}{1 - e^{-x^2}\alpha}\left[\frac{x^2}{2\pi^2\hbar^3}\left(\frac{2m}{\beta}\right)^{3/2}\right]dx = s\frac{1}{4\pi^2\hbar^3}\left(\frac{2m}{\beta}\right)^{3/2}\left[\int x^2\left(\alpha e^{-x^2}dx + \alpha^2 e^{-2x^2}dx + \ldots\right)\right]$$

1D *never converges*

$$= s\left(\frac{mk_BT}{2\pi\hbar^2}\right)^{3/2}\left(\alpha + \frac{\alpha^2}{2^{3/2}} + \frac{\alpha^3}{3^{3/2}} + \ldots\right) = s\left(\frac{mk_BT}{2\pi\hbar^2}\right)^{3/2}\zeta_{3/2}(\alpha). \qquad \alpha = e^{\beta\mu}\ (\leq 1)$$

1/2 1/2 1/2

1D

$$\frac{\langle N\rangle}{V} = \rho = s\left(\frac{mk_BT_c}{2\pi\hbar^2}\right)^{3/2}\cdot\zeta_{3/2}(1), \quad T_c = \frac{2\pi\hbar^2}{mk_B}\left(\frac{\rho/s}{\zeta_{3/2}(1)}\right)^{2/3}$$

$$\zeta_{3/2}(1) = 1 + \frac{1}{2^{3/2}} + \frac{1}{3^{3/2}} + \ldots = 2{,}612$$

$$\langle n_0\rangle = \langle N\rangle\left[1 - \left(\frac{T}{T_c}\right)^{3/2}\right]$$

Strong Coupling:

$\varepsilon \rightarrow \hbar^2k_Z^2/2M + X(F,k_Z = 0)$

$\alpha \rightarrow Exp[-(2\gamma_0/k_BT)\,X(F_C,0)]$

DOES CONVERGE !!

$\langle n_1(k_Z = 0)\rangle = \langle n_1\rangle(1 - T/T_C)$

$T < T_C = (2\gamma_0/k_B)\,X(F_C,0)$

I.V.Bondarev & A.V.Meliksetyan, Phys. Rev. B 89, 045414 (2014)

POSSIBILITY FOR EXCITON BEC BY MEANS OF CONTROLLED COUPLING TO INTER-BAND PLASMONS

(*via the Quantum Confined Stark Effect*)

Critical Temperature

$$T_C = \left(2\gamma_0 / k_B\right) X\left(F, k_Z = 0\right)$$

$$\gamma_0 = 2.7 \text{ eV}$$

Exciton Ratio Condensed

$$\left\langle n_1(k_Z = 0)\right\rangle \frac{N(Exciton)}{N(Plasmon)}$$

I.V.Bondarev, PRB 80, 085407 (2009)

Upper-Branch Exciton-Plasmon Fraction Condensed

$$\left\langle n_1(k_Z = 0)\right\rangle = \left\langle n_1\right\rangle \left(1 - T/T_C\right)$$

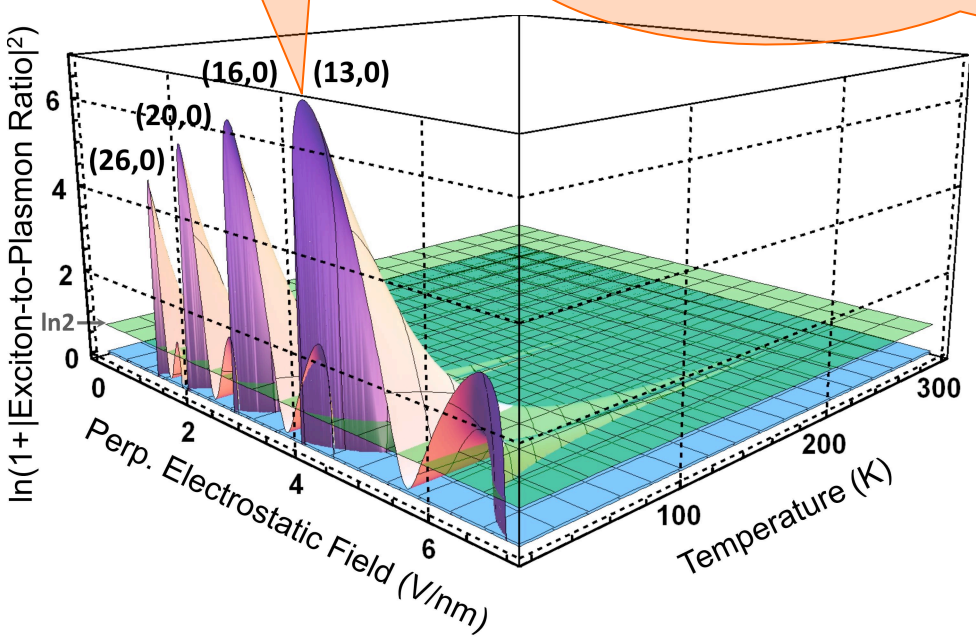

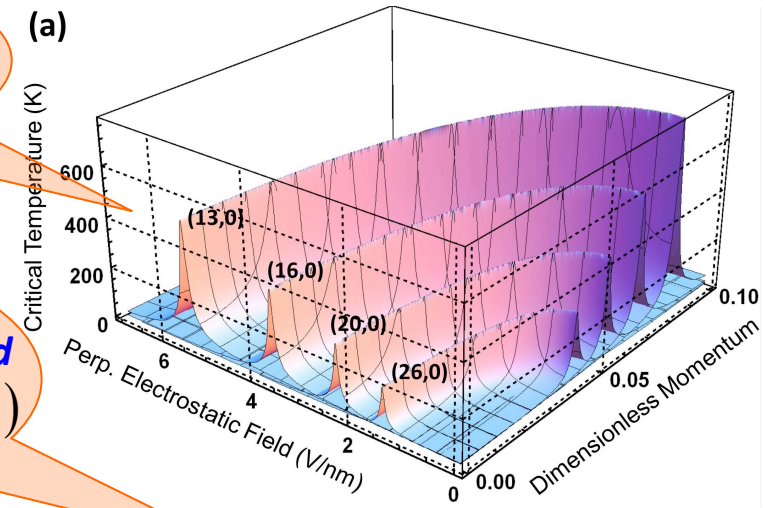

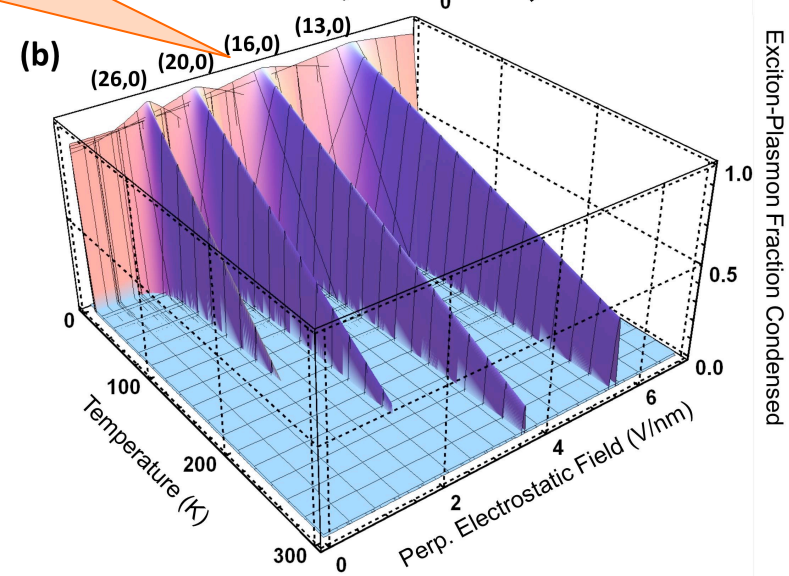

I.V.Bondarev, KITP [flectro22] Seminar, 08/01/22

I.V.Bondarev & A.V.Meliksetyan, Phys. Rev. B 89, 045414 (2014)

RELEVANCE OF THE EXCITON BEC PRESENTED HERE TO EARLIER STUDIES OF BEC IN LOW-DIMENSIONAL SYSTEMS

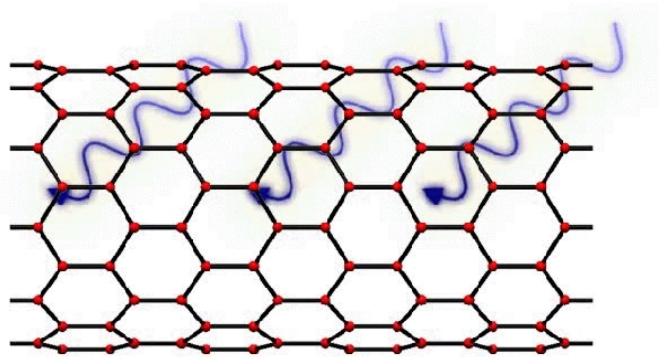

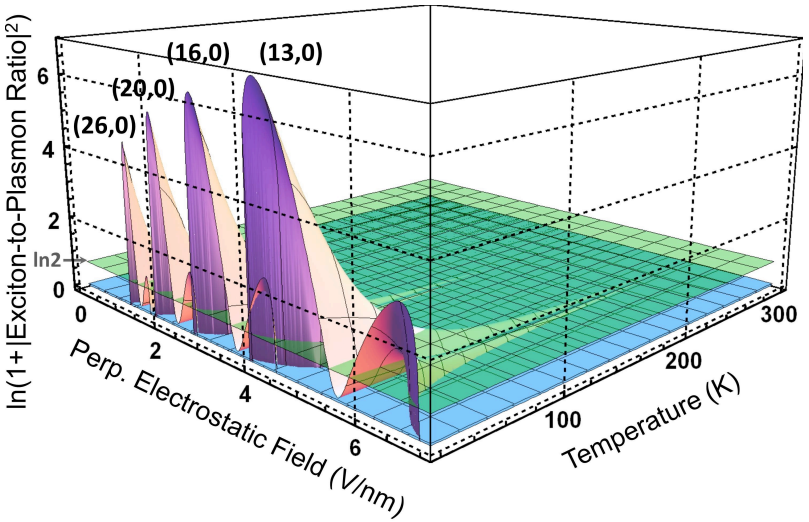

PHYSICAL REVIEW A VOLUME 44, NUMBER 11 1 DECEMBER 1991

Bose-Einstein condensation in low-dimensional traps

Vanderlei Bagnato
Instituto de Fisica e Quimica de Sao Carlos, Caixa Postal 369, 13560 Sao Carlos, São Paulo, Brazil

Daniel Kleppner
Department of Physics, Massachusetts Institute of Technology, Cambridge, Massachusetts 02139
(Received 8 April 1991)

We demonstrate the possibility of Bose-Einstein condensation (BEC) of an ideal Bose gas confined by one- and two-dimensional power-law traps. One-dimensional systems display BEC in traps that are more confining than parabolic: $U(x) \sim x^{\eta}, \eta < 2$. Two-dimensional systems display BEC for any finite value of η. A possible experimental configuration for a two-dimensional trap is described.

PACS number(s): 32.80.Pj, 05.30.Jp, 67.65.+z, 64.60.−i

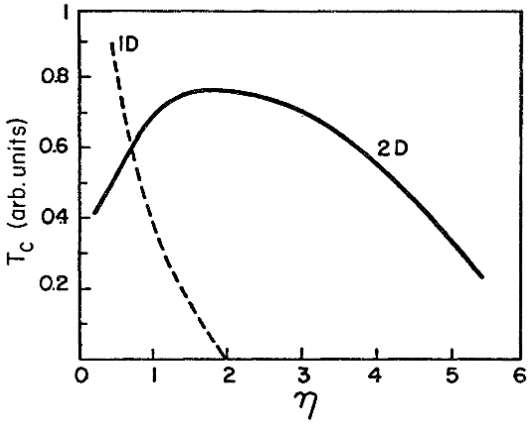

OUTLINE

- ***Pristine Semiconducting Carbon Nanotubes:***
  Excitons and Interband Plasmons – Brief Review

- ***Plasmon Generation by Optically Excited Excitons, Exciton BEC Effect***

- ***Excitonic Complexes (Biexcitons & Trions) in quasi-1D:***
  Brief Review, Understand Their Relative Stability

- ***Hybrid Carbon Nanotube Systems:*** ***Plasmon Enhanced Raman Scattering Effect, Transmission Fano Resonances in Hybrid Metal-Encapsulating Semiconducting CNs, CN arrays***

- ***Summary***

EXPERIMENT & THEORY

Charged and Neutral Excitonic Complexes in Confined Semiconductors
Role of Quantum Confinement

PHYSICAL REVIEW B **70**, 035323 (2004)

Influence of well-width fluctuations on the binding energy of excitons, charged excitons, and biexcitons in GaAs-based quantum wells

A. V. Filinov,[1,2,3] C. Riva,[1] F. M. Peeters,[1] Yu. E. Lozovik,[2] and M. Bonitz[3]
[1]*Departement Natuurkunde, Universiteit Antwerpen (Drie Eiken Campus), Universiteitsplein 1, B-2610 Antwerpen, Belgium*
[2]*Institute of Spectroscopy RAS, Moscow region, Troisk 142190, Russia*
[3]*Christian-Albrechts-Universität zu Kiel, Institut für Theoretische Physik und Astrophysik, Leibnizstrasse 15, 24098 Kiel, Germa*
(Received 19 January 2004; revised manuscript received 8 April 2004; published 28 July 2004)

We present a first-principle path integral Monte Carlo (PIMC) study of the binding energy of excitons, trions (positively and negatively charged excitons) and biexcitons bound to single-island interface defects in quasi-two-dimensional $GaAs/Al_xGa_{1-x}As$ quantum wells. We discuss in detail the dependence of the binding energy on the size of the well-width fluctuations and on the quantum-well width. The numerical results for the well-width dependence of the exciton, trions and biexciton binding energy are in good quantitative agreement with the available experimental data.

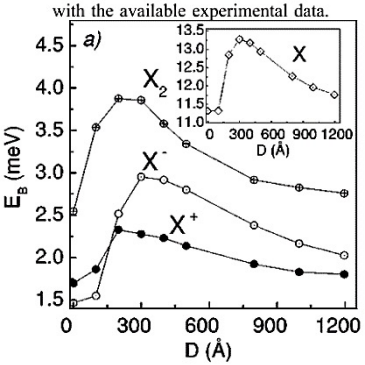

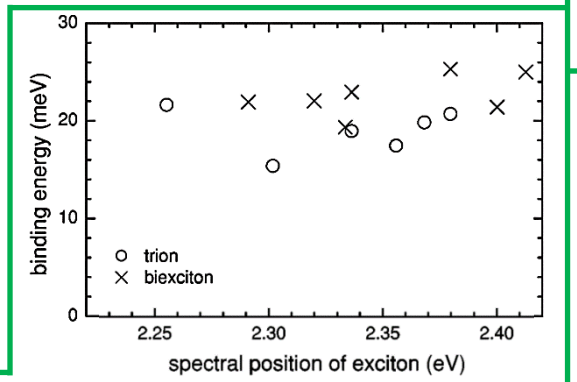

PHYSICAL REVIEW B **68**, 125316 (2003)

Trion, biexciton, and exciton dynamics in single self-assembled CdSe quantum dots

B. Patton, W. Langbein, and U. Woggon*
Experimentelle Physik IIb, Universität Dortmund, Otto-Hahn-Str. 4, 44221 Dortmund, Germany
(Received 7 February 2003; published 18 September 2003)

We present an analysis of time- and polarization-resolved data taken in microphotoluminescence experiments on individual CdSe/ZnSe quantum dots grown by molecular beam epitaxy. The identification of individual dots was performed by a spectral jitter correlation technique and by their polarization properties and density dependences. Decay times are given for exciton, trion, and biexciton states and evidence is shown for a spin-relaxation-limited energy relaxation of the trion. For the bright-exciton state the temperature dependence of the decay time is studied and a repopulation from the dark-exciton state is observed. Trion binding energies of 15–22 meV and biexciton binding energies of 19–26 meV are found.

PHYSICAL REVIEW B VOLUME 58, NUMBER 4 15 JULY 1998-II

Biexcitons in semiconductor quantum wires

T. Baars, W. Braun, M. Bayer, and A. Forchel
Technische Physik, Universität Würzburg, Am Hubland, 97074 Würzburg, Germany
(Received 19 November 1997; revised manuscript received 4 May 1998)

We report on spectrally resolved four-wave mixing experiments on $In_xGa_{1-x}As/GaAs$ quantum wires for a wide range of lateral sizes. Due to the polarization dependence of the four-wave mixing signal, beats in the decay of the signal and an additional emission line in the four-wave mixing spectrum can be clearly attributed to biexcitons. We find that the biexciton binding energy depends on both the vertical and lateral dimensions of the wires. For quantum wires with a large vertical confinement we observe an enhancement of the binding energy of about 40% as compared to a two-dimensional reference sample whereas the biexciton binding energy is found to be wire width independent in wires with shallow vertical confinement. [S0163-1829(98)52328-4]

	$E^B_{X^-}$	$E^B_{X^+}$
Thin (Theor.)	2.25	2.85
Thick (Theor.)	1.29	1.6

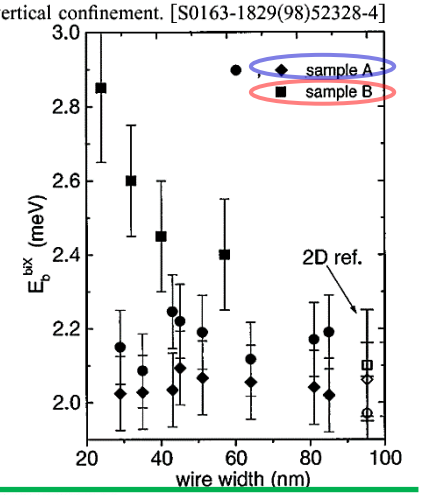

PHYSICAL REVIEW B **77**, 205413 (2008)

Influence of the shape and size of a quantum wire on the trion binding energy

Y. Sidor, B. Partoens,* and F. M. Peeters†
Departement Fysica, Universiteit Antwerpen, Groenenborgerlaan 171, B-2020 Antwerpen, Belgium
(Received 19 December 2007; revised manuscript received 11 April 2008; published 12 May 2008)

The binding energy for charged excitons (X^- and X^+) is calculated within the single-band effective mass approximation including effects due to strain for rectangular, triangular, and V-shaped quantum wires. Both X^- and X^+ are found to be bound in rectangular InAs/InP quantum wires and V-shaped $GaAs/Al_{0.32}Ga_{0.68}As$ quantum wires. We found an appreciable dependence of the trion binding energy on the size and shape of the quantum wire. We compare with available experimental data.

RECENT EXPERIMENTS

Charged and Neutral Excitonic Complexes in CNs

B.Yuma et al., Phys. Rev. B 87, 205412 (2013)
L.Colombier et al., Phys. Rev. Lett. 109, 197402 (2012)
R.Matsunaga et al., Phys. Rev. Lett. 106, 037404 (2011)

PHYSICAL REVIEW B **87**, 205412 (2013)

Biexciton, single carrier, and trion generation dynamics in single-walled carbon nanotubes

B. Yuma,[1] S. Berciaud,[1] J. Besbas,[1] J. Shaver,[2] S. Santos,[2] S. Ghosh,[3] R. B. Weisman,[3] L. Cognet,[2] M. Gallart,[1] M. Ziegler,[1] B. Hönerlage,[1] B. Lounis,[2] and P. Gilliot[1,*]
[1]*IPCMS, CNRS and Université de Strasbourg, 23, rue du Læss, F-67034 Strasbourg, France*
[2]*LP2N, Université de Bordeaux, Institut d'Optique Graduate School, and CNRS, 351 cours de la Libération, F-33405 Talence, France*
[3]*Department of Chemistry and R. E. Smalley Institute for Nanoscale Science and Technology, Rice University, 6100 Main Street, Houston, Texas 77005, USA*
(Received 6 February 2013; published 8 May 2013)

We present a study of free carrier photogeneration and multicarrier bound states, such as biexcitons and trions (charged excitons), in semiconducting single-walled carbon nanotubes. Pump-and-probe measurements performed with fs pulses reveal the effects of strong Coulomb interactions between carriers on their dynamics. Biexciton formation by optical transition from exciton population results in an induced absorption line (binding energy 130 meV). Exciton-exciton annihilation process is shown to evolve at high densities towards an Auger process that can expel carriers from nanotubes. The remaining carriers give rise to an induced absorption due to trion formation (binding energy 190 meV). These features show the dynamics of exciton and free carriers populations.

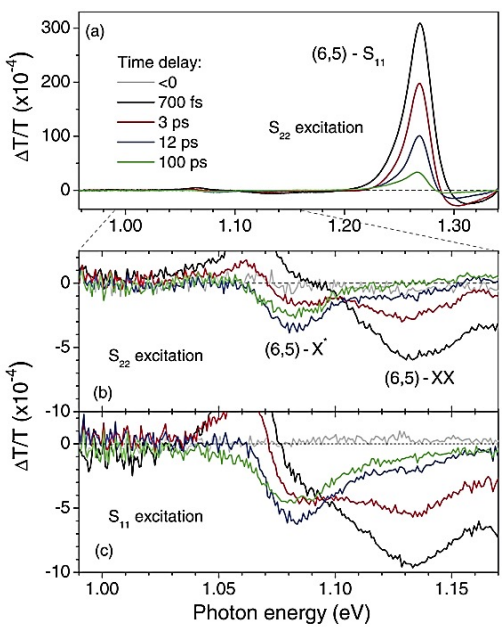

Selected for a Viewpoint in *Physics*
PRL **106,** 037404 (2011) PHYSICAL REVIEW LETTERS week ending 21 JANUARY 2011

Observation of Charged Excitons in Hole-Doped Carbon Nanotubes Using Photoluminescence and Absorption Spectroscopy

Ryusuke Matsunaga,[1] Kazunari Matsuda,[1] and Yoshihiko Kanemitsu[1,2]
[1]*Institute for Chemical Research, Kyoto University, Uji, Kyoto 611-0011, Japan*
[2]*Photonics and Electronics Science and Engineering Center, Kyoto University, Kyoto 615-8510, Japan*
(Received 13 September 2010; published 18 January 2011)

We report the first observation of trions (charged excitons), three-particle bound states consisting of one electron and two holes, in hole-doped carbon nanotubes at room temperature. When *p*-type dopants are added to carbon nanotube solutions, the photoluminescence and absorption peaks of the trions appear far below the E_{11} bright exciton peak, regardless of the dopant species. The unexpectedly large energy separation between the bright excitons and the trions is attributed to the strong electron-hole exchange interaction in carbon nanotubes.

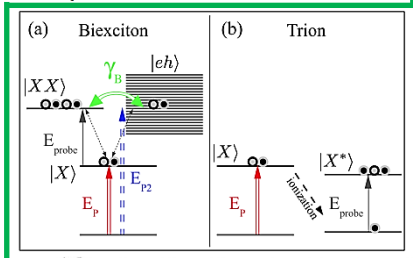

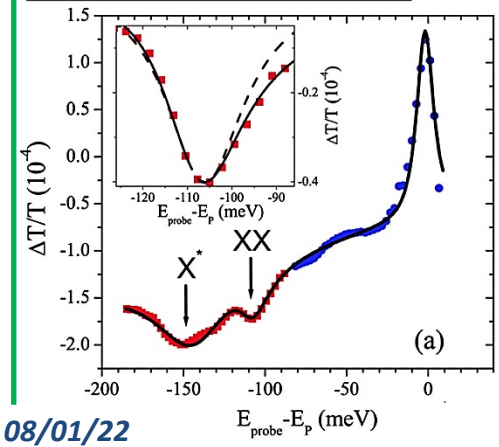

PRL **109,** 197402 (2012) PHYSICAL REVIEW LETTERS week ending 9 NOVEMBER 2012

Detection of a Biexciton in Semiconducting Carbon Nanotubes Using Nonlinear Optical Spectroscopy

L. Colombier,[1,2] J. Selles,[1,2] E. Rousseau,[1,2] J. S. Lauret,[3] F. Vialla,[4] C. Voisin,[4] and G. Cassabois[1,2,*]
[1]*Laboratoire Charles Coulomb UMR5221, Université Montpellier 2, F-34095 Montpellier, France*
[2]*Laboratoire Charles Coulomb UMR5221, CNRS, F-34095 Montpellier, France*
[3]*LPQM-ENS-Cachan, 61 Avenue du Président Wilson, 94235 Cachan Cedex, France*
[4]*Laboratoire Pierre Aigrain, Ecole Normale Supérieure, UPMC, Université Paris Diderot, CNRS UMR8551, 24 rue Lhomond, 75231 Paris Cedex 5, France*
(Received 17 July 2012; published 7 November 2012)

We report the observation of the biexciton in semiconducting single-wall carbon nanotubes by means of nonlinear optical spectroscopy. Our measurements reveal the universal asymmetric line shape of the Fano resonance intrinsic to the biexciton transition. For nanotubes of the (9,7) chirality, we find a biexciton binding energy of 106 meV. From the calculation of the $\chi^{(3)}$ nonlinear response, we provide a quantitative interpretation of our measurements, leading to an estimation of the characteristic Fano factor q of 7 ± 3. This value allows us to extract the first experimental information on the biexciton stability and we obtain a biexciton annihilation rate comparable to the exciton-exciton annihilation one.

Also trion binding energy of 150 meV reported

BIEXCITON

Biexciton Binding Energy within the Landau-Herring Approach

Landau, Quantum Mechanics; C.Herring, Rev. Mod. Phys. 34, 631 (1962)
MODEL developed: I.V.Bondarev, Phys. Rev. B 83, 153409 (2011)

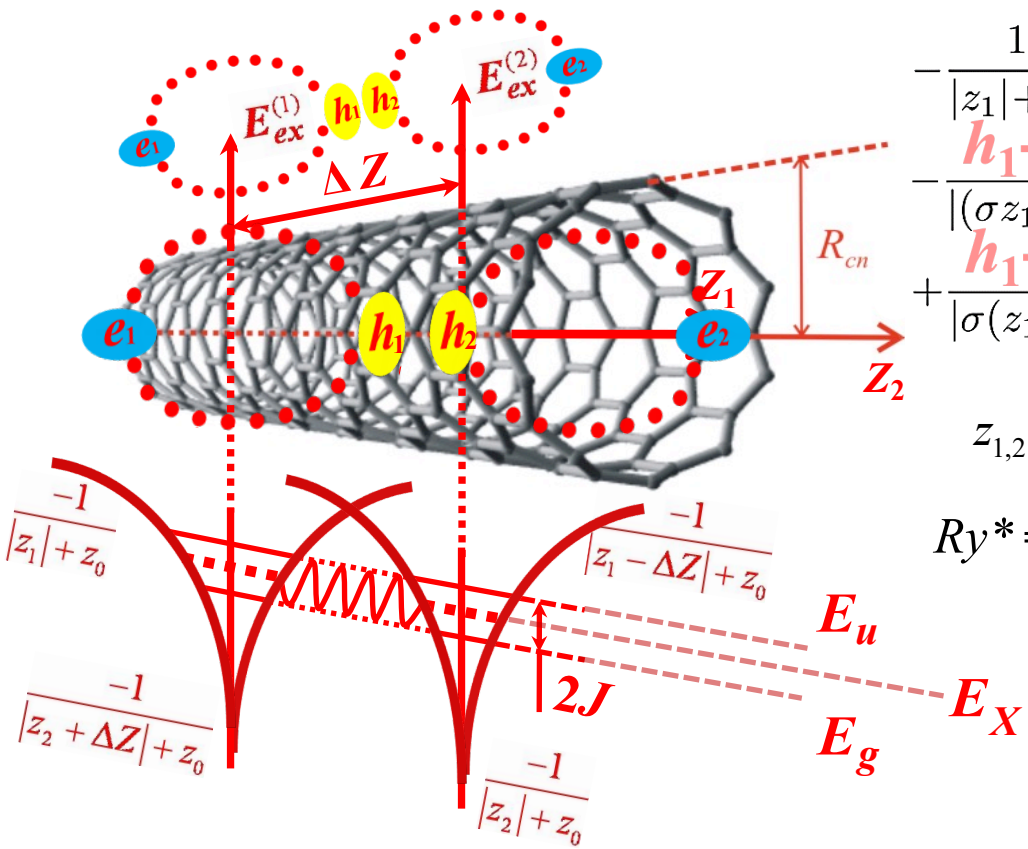

$$\hat{H}(z_1,z_2,\Delta Z) = -\frac{\partial^2}{\partial z_1^2} - \frac{\partial^2}{\partial z_2^2}$$

$$-\frac{1}{|z_1|+z_0} - \frac{1}{|z_1-\Delta Z|+z_0} - \frac{1}{|z_2|+z_0} - \frac{1}{|z_2+\Delta Z|+z_0}$$

$$-\frac{2}{|(\sigma z_1+z_2)/\lambda+\Delta Z|+z_0} - \frac{2}{|(z_1+\sigma z_2)/\lambda-\Delta Z|+z_0}$$

$$+\frac{2}{|\sigma(z_1-z_2)/\lambda+\Delta Z|+z_0} + \frac{2}{|(z_1-z_2)/\lambda-\Delta Z|+z_0}$$

h_1-e_2 h_2-e_1 h_1-h_2 e_1-e_2

$$z_{1,2} = z_{e1,2} - z_{h1,2};\ \lambda = 1+\sigma;\ \sigma = m_e/m_h \to 1$$

due to the mass reversal effect

$$Ry^* = \frac{\hbar^2}{2\mu a_B^{*2}} = \frac{\mu(\text{in } m_0)}{\varepsilon^2}13.6\text{ eV};\ a_B^* = \frac{\varepsilon}{\mu}0.529\,\text{Å}$$

Biexciton Binding Energy

$$E_{XX} = E_g - 2E_X = -J_{XX}(\Delta Z_0)$$

TRION

Trion Binding Energy within the Landau-Herring Approach

Landau, Quantum Mechanics; C.Herring, Rev. Mod. Phys. 34, 631 (1962)
MODEL developed: I.V.Bondarev, Phys. Rev. B 90, 245430 (2014)

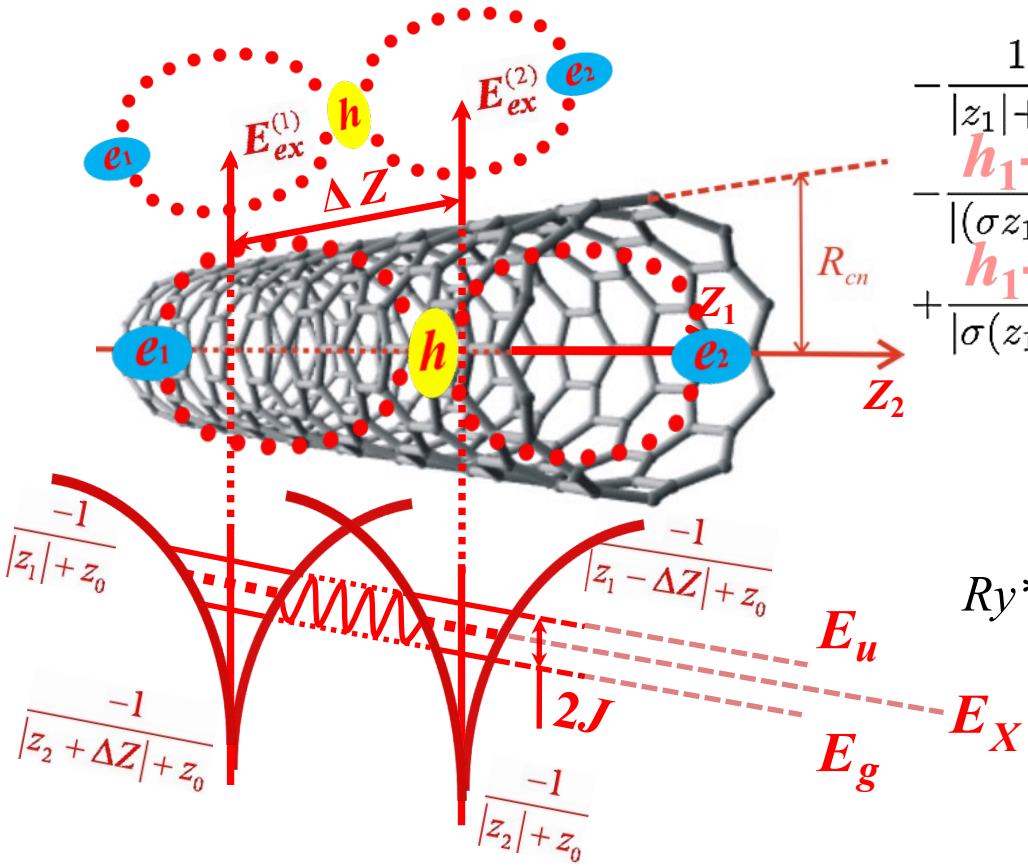

$$\hat{H}(z_1,z_2,\Delta Z) = -\frac{\partial^2}{\partial z_1^2} - \frac{\partial^2}{\partial z_2^2} - \frac{1}{|z_1|+z_0} - \frac{1}{|z_1-\Delta Z|+z_0} - \frac{1}{|z_2|+z_0} - \frac{1}{|z_2+\Delta Z|+z_0}$$

$$- \frac{2}{|(\sigma z_1+z_2)/\lambda+\Delta Z|+z_0} - \frac{2}{|(z_1+\sigma z_2)/\lambda-\Delta Z|+z_0}$$

$$+ \frac{2}{|\sigma(z_1-z_2)/\lambda+\Delta Z|+z_0} + \frac{2}{|(z_1-z_2)/\lambda-\Delta Z|+z_0}$$

h_1-e_2 h_2-e_1 h_1-h_2 e_1-e_2

positive trion $z_{1,2} = z_e - z_{h1,2}$

negative trion $z_{1,2} = z_{e1,2} - z_h$

$$\lambda = 1+\sigma; \quad \sigma = m_e/m_h \to 1$$

due to the mass reversal effect

$$Ry^* = \frac{\hbar^2}{2\mu a_B^{*2}} = \frac{\mu(\text{in } m_0)}{\varepsilon^2} 13.6\,\text{eV}; \quad a_B^* = \frac{\varepsilon}{\mu} 0.529\,\text{Å}$$

Trion Binding Energy

$$E_{X^*} = E_g - 2E_X = -J_{X^*}(\Delta Z_0)$$

BIEXCITON & TRION

in the Configuration Space of Two Independent Relative e-h Coordinates

I.V.Bondarev, Phys. Rev. B 83, 153409 (2011)
I.V.Bondarev, Phys. Rev. B 90, 245430 (2014)

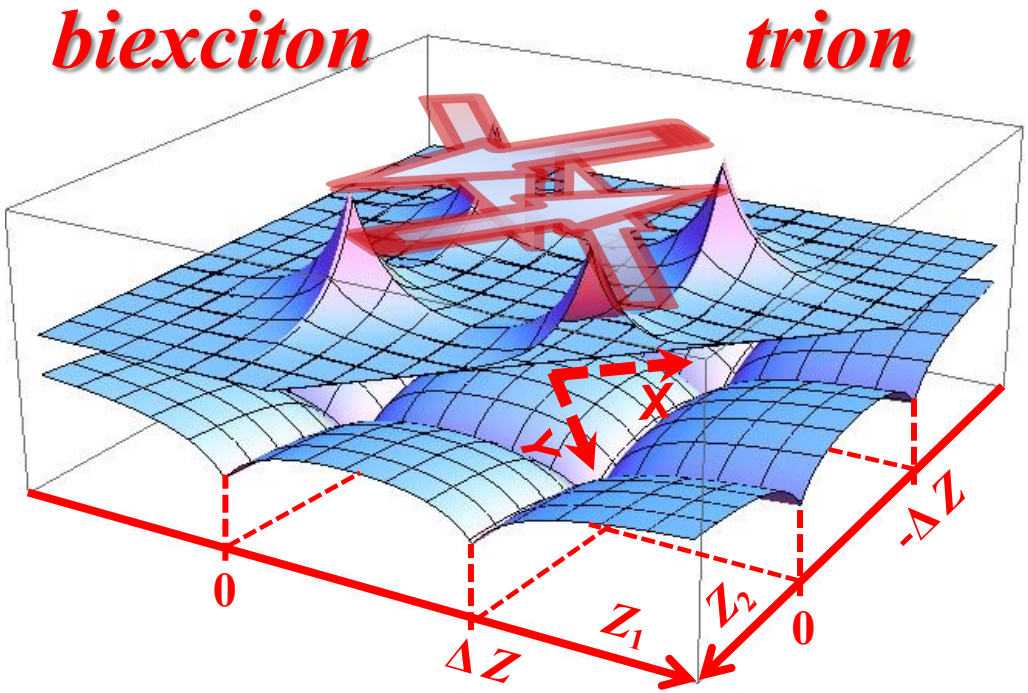

Biexciton Binding Energy

$$E_{XX} = -\frac{1}{9}\left|E_X\right|\left(\frac{e}{3}\right)^{2\sqrt{Ry^*/|E_X|}-1}$$

Trion Binding Energy

$$E_{X^*} = -\frac{1}{e}\left|E_X\right|2^{-2\sqrt{Ry^*/|E_X|}}$$

Trion/Biexciton Ratio

$$\frac{E_{X^*}}{E_{XX}} = 3\left(\frac{3}{2e}\right)^{2\sqrt{Ry^*/|E_X|}}$$

$$J_{XX}(\Delta Z) = \frac{2}{3!}\int_{-\Delta Z/\sqrt{2}}^{\Delta Z/\sqrt{2}}\left|\psi_{XX}(x,y)\frac{\partial\psi_{XX}(x,y)}{\partial x}\right|_{x=0} dy$$

$$J_{X^*}(\Delta Z) = \int_{-\Delta Z/\sqrt{2}}^{\Delta Z/\sqrt{2}}\left|\psi_{X^*}(x,y)\frac{\partial\psi_{X^*}(x,y)}{\partial x}\right|_{x=0} dy$$

$$Ry^* = \frac{\hbar^2}{2\mu a_B^{*2}} = \frac{\mu(\text{in } m_0)}{\varepsilon^2}13.6\text{ eV};\quad a_B^* = \frac{\varepsilon}{\mu}0.529\,\text{Å}$$

BINDING ENERGY DEPENDENCE ON THE CN DIAMETER, EFFECTIVE MASS, AND DIELECTRIC CONSTANT

I.V.Bondarev, Phys. Rev. B 90, 245430 (2014)

$$Ry^* = \frac{\mu}{\varepsilon^2} 13.6\,\text{eV}; \quad a_B^* = \frac{\varepsilon}{\mu} 0.529\,\text{Å}$$

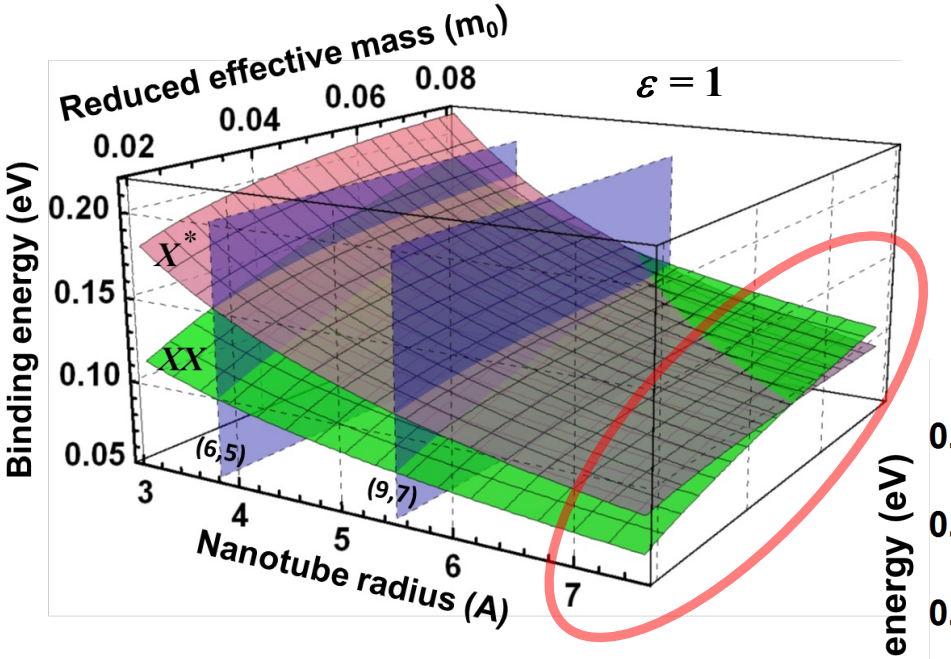

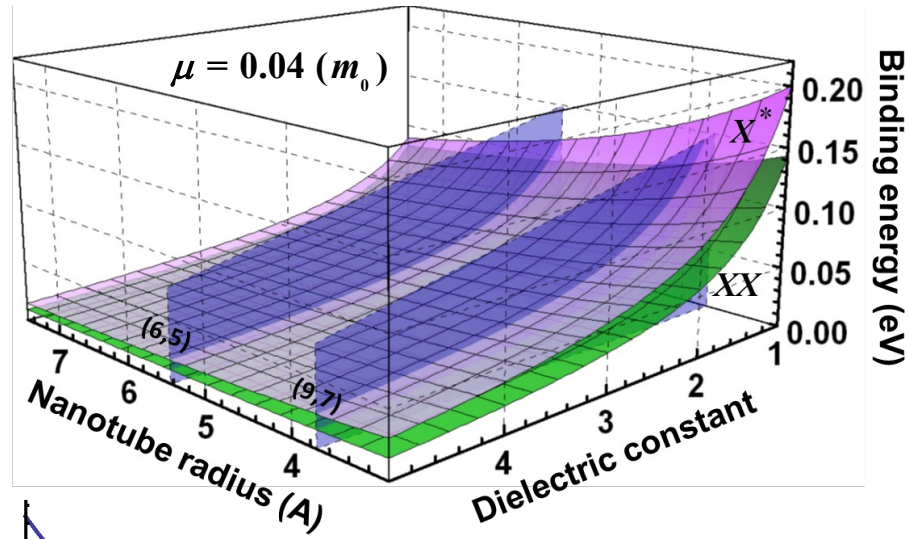

$$\varepsilon = 1, \;\; \mu = 0.04\,(m_0) \quad \Rightarrow$$

***CNs in air** [or in a dielectric, for the lowest excitation energy ground-state exciton <u>only</u>]*

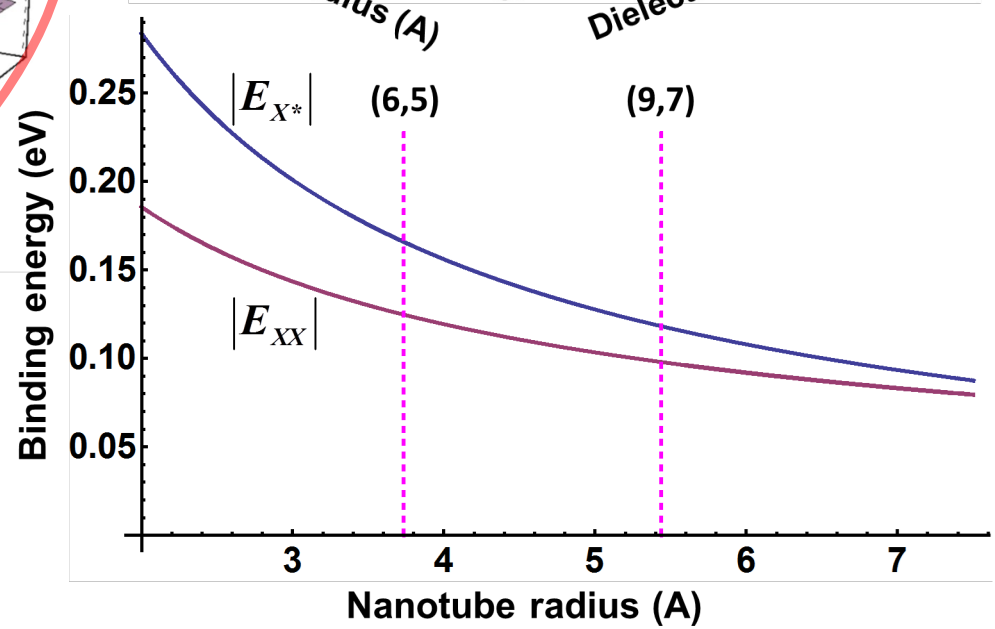

OUTLINE

- ***Pristine Semiconducting Carbon Nanotubes:***
  Excitons and Interband Plasmons – Brief Review

- ***Plasmon Generation by Optically Excited Excitons, Exciton BEC Effect***

- ***Excitonic Complexes (Biexcitons & Trions) in quasi-1D:***
  Brief Review, Understanding Relative Stability

- ***Hybrid Carbon Nanotube Systems: Plasmon Enhanced Raman Scattering Effect, Transmission Fano Resonances in Hybrid Metal-Encapsulating Semiconducting CNs***

- ***Summary***

INTERBAND PLASMONS OF CARBON NANOTUBES ARE SIMILAR TO CAVITY PHOTONS IN MICROCAVITY SYSTEMS

I.V.Bondarev & Ph.Lambin, Phys. Rev. B 72, 035451 (2005);
also Ch.6, pp.139-183 in "Trends in Nanotubes Research" (Nova Science, 2006)

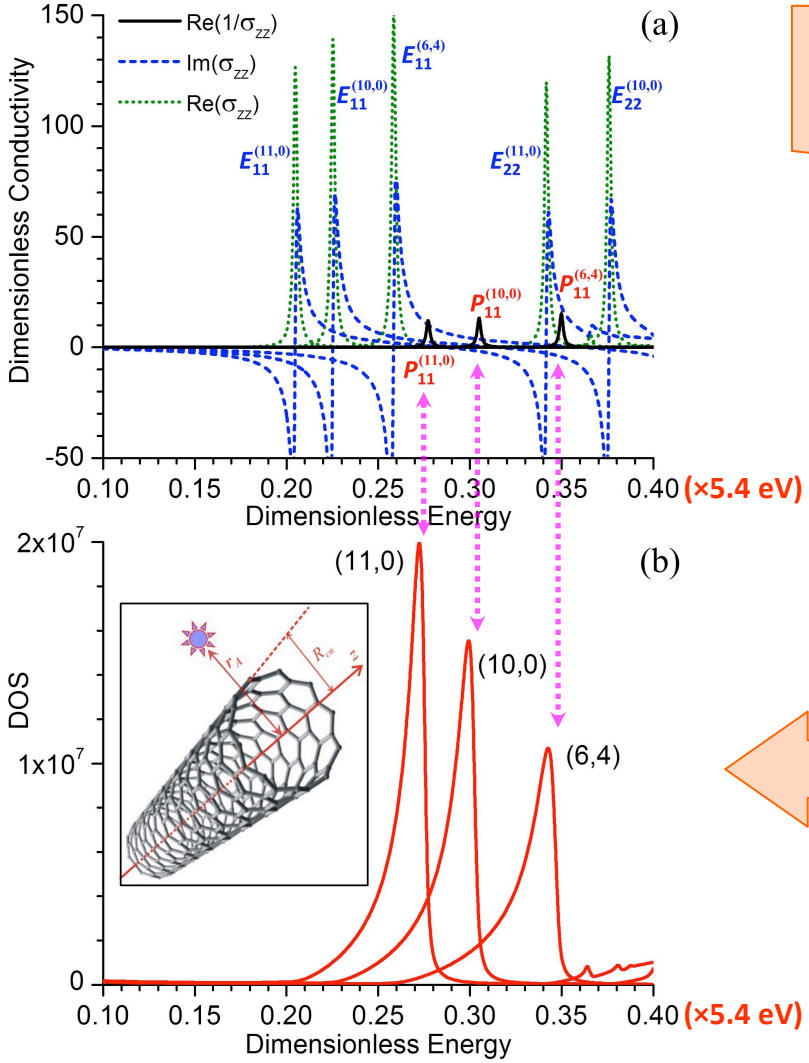

Local Density of Photonic States (DOS) for a two-level emitter coupled to ⊥ (||)-polarized electromagnetic field (same as Purcell factor)

$$\xi^{\perp(\|)}(\mathbf{r}_A,\omega) = \frac{\mathrm{Im}^{\perp(\|)} G_{zz}^{\perp(\|)}(\mathbf{r}_A,\mathbf{r}_A,\omega)}{\mathrm{Im} G_{zz}^{0}(\omega)}$$

$$\xi^{\perp}(r_A \sim R_{CN},\omega) = \xi^{\|}(r_A \sim R_{CN},\omega) = \xi$$

$$\xi = \frac{\Gamma(r_A,\omega)}{\Gamma_0(\omega)}, \quad \Gamma_0 = \frac{4 d_z^2 \omega^3}{3\hbar c^3} = \Gamma_{vac}$$

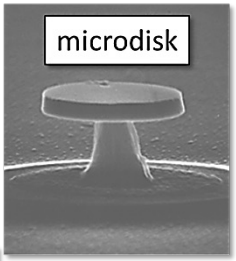

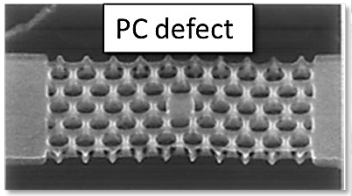

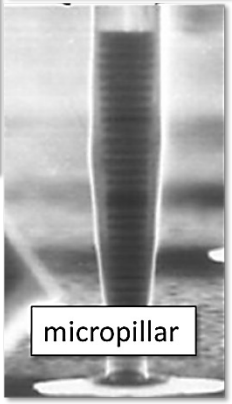

$$F_{Purcell} = \frac{\Gamma_{cav}}{\Gamma_{vac}} = \frac{3\lambda^3}{4\pi^2 n^3}\left(\frac{Q}{V_{cav}}\right)$$

J.M.Gerard, in: ***Single Quantum Dots****, P.Michler, ed., Topics Appl. Phys. 90, 269–315 (2003)*

THE MODEL: FOUR-LEVEL SYSTEM OF A TWO-LEVEL ATOM COUPLED TO AN INTERBAND PLASMON RESONANCE

I.V.Bondarev, Optics Express 23, 3971 (2015)

4-level system of a 2-level atom coupled to a plasmon resonance. General case

$$
\begin{aligned}
|0\rangle &= |l\rangle|\{0\}\rangle, \\
|1,2\rangle &= C_u^{(1,2)}|u\rangle|\{0\}\rangle + \int_0^\infty d\omega \int d\mathbf{R}\, C_l^{(1,2)}(\mathbf{R},\omega)|l\rangle|\{1(\mathbf{R},\omega)\}\rangle, \\
|3\rangle &= |u\rangle|\{1(\mathbf{R},\omega)\}\rangle.
\end{aligned}
$$

$$
C_u^{(1,2)} = \left[\frac{1}{2}\left(1 + \frac{1 \mp \sqrt{1+X^2/\delta^2}}{1+X^2/\delta^2 \mp \sqrt{1+X^2/\delta^2}}\right)\right]^{1/2},
$$

$$
\varepsilon_0 = -\frac{\tilde{x}_A}{2}, \quad \varepsilon_{1,2} = \frac{1}{2}\left(x_p \mp \sqrt{\delta^2+X^2} - i\Delta x_p\right), \quad \varepsilon_3 = \frac{\tilde{x}_A}{2} + x_p - i\Delta x_p
$$

$$
\varepsilon_i = E_i/2\gamma_0 \ (i=0,1,2,3),\ \gamma_0 = 2.7\,\text{eV},\ (\tilde{x}_A, x_p, \Delta x_p) = \hbar(\tilde{\omega}_A, \omega_p, \Delta\omega_p)/2\gamma_0
$$

$$
\delta = \tilde{x}_A - x_p,\ X = (\hbar/2\gamma_0)\left[2\Delta\omega_0\Gamma_0(\omega_p)(1+\omega_A^2/\omega_p^2)\xi(\mathbf{r}_A,\omega_p)\right]^{1/2}
$$

Fermi Golden Rule scattering probability

$$
\left(\frac{2\pi}{\hbar}\right)\left|\frac{\langle 0|\hat{H}_R(\omega_s)|1\rangle\langle 1|\hat{H}_{AF}^{(e)}|2\rangle\langle 2|\hat{H}_R(\omega_i)|0\rangle}{[\hbar\omega_i - \hbar\omega_p - (E_1-E_0)][\hbar\omega_i - (E_2-E_0)]}\right.
$$

$$
\left. + \frac{\langle 0|\hat{H}_R(\omega_i)|1\rangle\langle 1|\hat{H}_{AF}^{(e)}|2\rangle\langle 2|\hat{H}_R(\omega_s)|0\rangle}{[-\hbar\omega_s - \hbar\omega_p - (E_1-E_0)][-\hbar\omega_s - (E_2-E_0)]}\right|^2 \delta(\hbar\omega_i - \hbar\omega_p - \hbar\omega_s)
$$

$$
+ \left|\frac{\langle 0|\hat{H}_R(\omega_s)|2\rangle\langle 2|\hat{H}_{AF}^{(a)}|1\rangle\langle 1|\hat{H}_R(\omega_i)|0\rangle}{[\hbar\omega_i + \hbar\omega_p - (E_2-E_0)][\hbar\omega_i - (E_1-E_0)]}\right.
$$

$$
\left. + \frac{\langle 0|\hat{H}_R(\omega_i)|2\rangle\langle 2|\hat{H}_{AF}^{(a)}|1\rangle\langle 1|\hat{H}_R(\omega_s)|0\rangle}{[-\hbar\omega_s + \hbar\omega_p - (E_2-E_0)][-\hbar\omega_s - (E_1-E_0)]}\right|^2 \delta(\hbar\omega_i + \hbar\omega_p - \hbar\omega_s).
$$

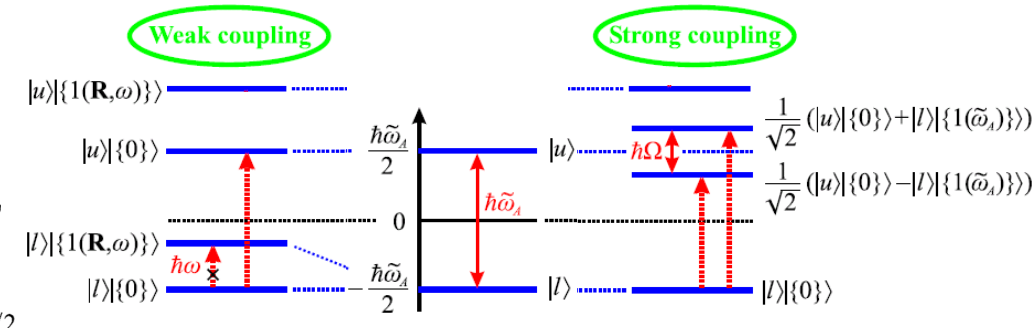

$$
|C_u^{(1,2)}|^2 + \int_0^\infty d\omega \int d\mathbf{R}\,|C_l^{(1,2)}(\mathbf{R},\omega)|^2 = 1
$$

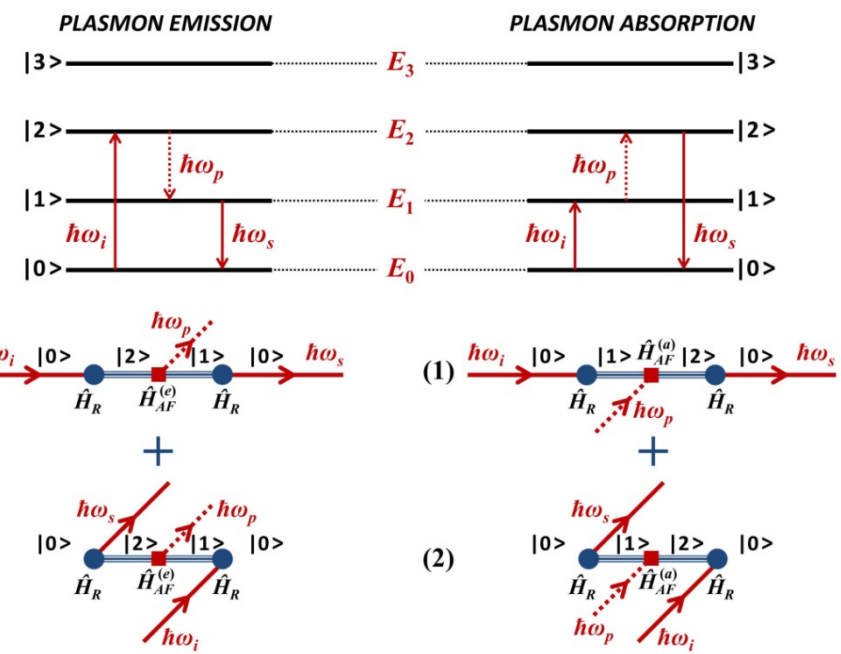

LIGHT SCATTERING BY A TWO-LEVEL EMITTER COUPLED TO AN INTERBAND PLASMON RESONANCE

Schematic illustration

Plasmon Emission

$\hbar\omega_s = \hbar\omega_i - \hbar\omega_p$

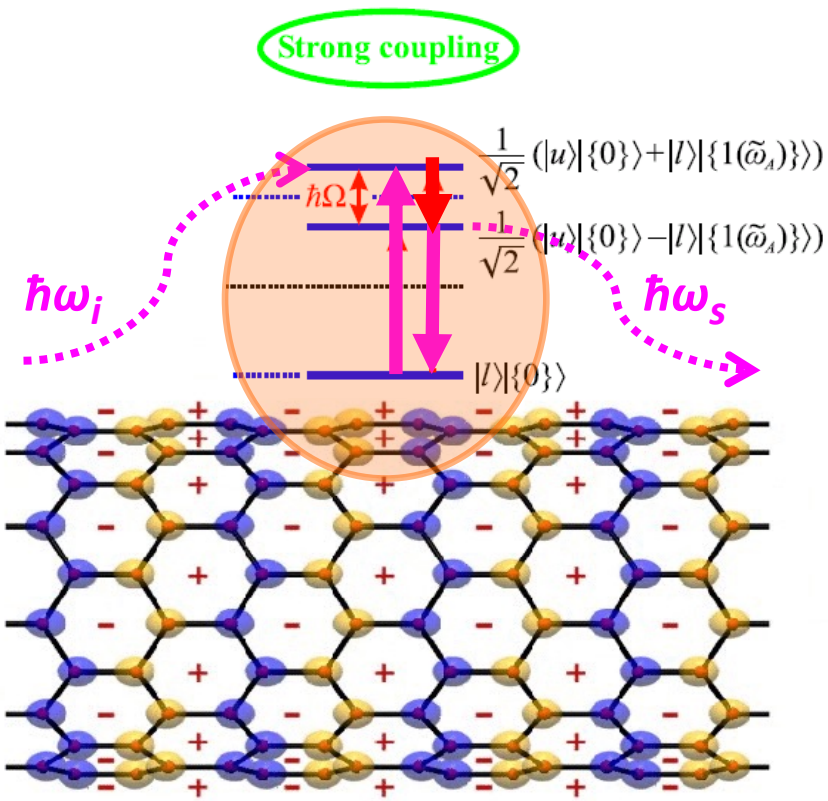

Plasmon Absorption

$\hbar\omega_s = \hbar\omega_i + \hbar\omega_p$

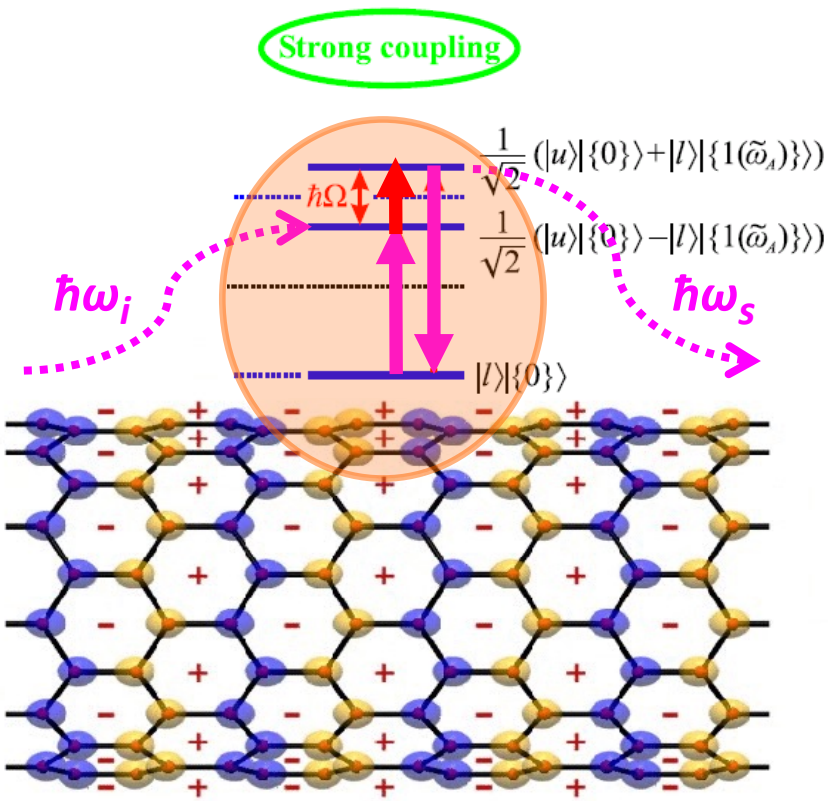

$$d_z E_z^{(loc)}(\mathbf{r}_A) \sim X \propto [\Gamma_0(\omega_p)\xi(\mathbf{r}_A,\omega_p)]^{1/2}$$

PLASMON ENHANCED RAMAN SCATTERING EFFECT FOR AN ATOM NEAR A CARBON NANOTUBE

Raman scattering cross-section. Enhancement factor

$$\frac{d\sigma}{d\Omega_s} = \frac{(2\gamma_0)^2|d_z|^4}{\hbar^4 c^4}\cos^2\vartheta_i\cos^2\vartheta_s P(x_i,x_s)\,, \quad x_{i,s} = \hbar\omega_{i,s}/2\gamma_0, \quad \cos\theta_{i,s} = \mathbf{e}_{i,s}\cdot\mathbf{e}_z$$

$$P(x_i,x_s) = x_i x_s^3 A(\delta,X,\Delta x_p)\left\{\frac{1}{[(x_i-x_p-\delta_+/2)^2+\Delta x_p^2][(x_s-x_p-\delta_-/2)^2+\Delta x_p^2]}\right.$$

$$\left.+\frac{1}{[(x_i-x_p-\delta_-/2)^2+\Delta x_p^2][(x_s-x_p-\delta_+/2)^2+\Delta x_p^2]}\right\}, \qquad \delta_\pm = \delta \pm \sqrt{\delta^2+X^2}$$

$$A(\delta,X,\Delta x_p) = \frac{X^8}{2^6(\delta^2+X^2)^2(\delta_-^2+\Delta x_p^2)} \sim [d_z E_z^{(loc)}(\mathbf{r}_A)]^4 \propto \xi^2(\mathbf{r}_A,\omega_p)$$

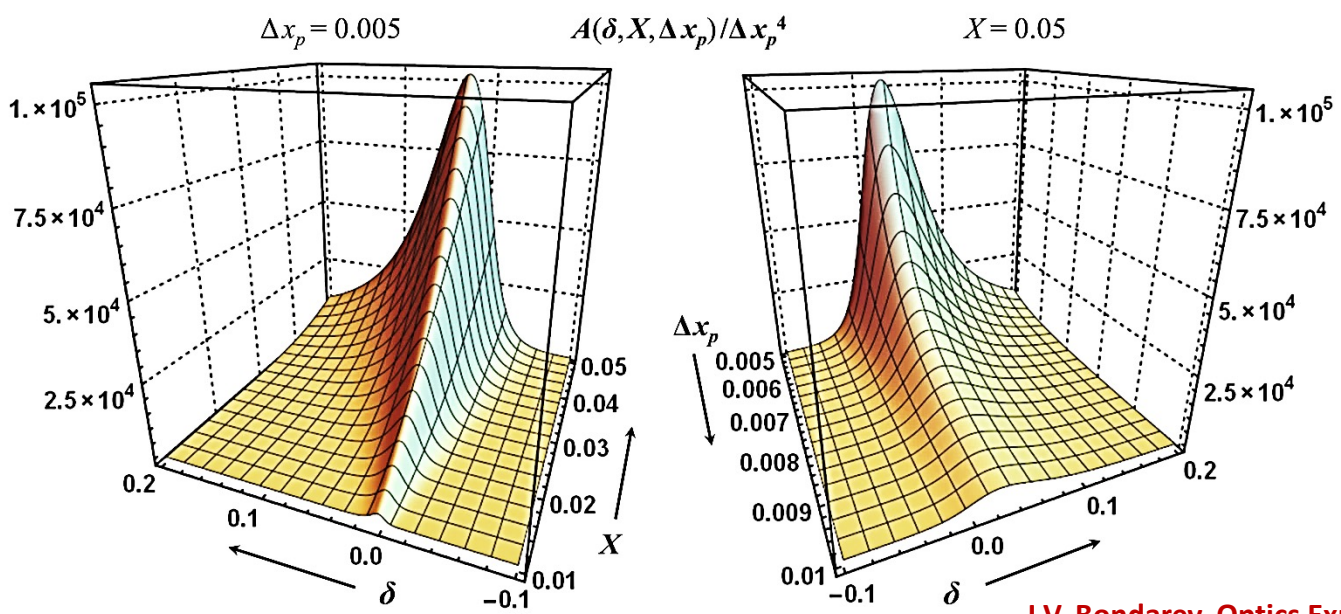

I.V. Bondarev, Optics Express 23, 3971 (2015)

HYBRID NANOSTRUCTURES OF CARBON NANOTUBES ENCAPSULATING METALLIC NANOWIRES

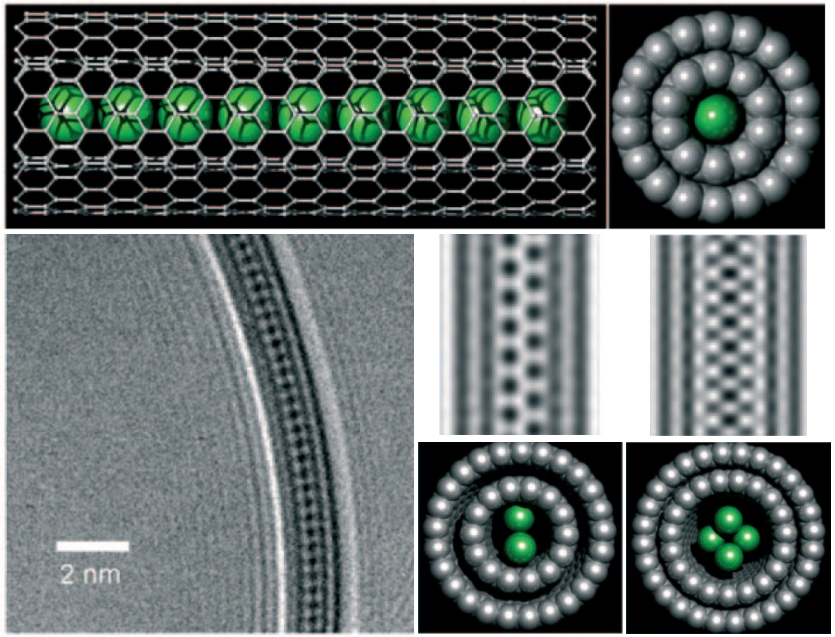

H.SHINOHARA group, JAPAN, Nagoya University-Chemistry:

R.Kitaura, et al., Angew. Chem. Int. Ed. 48, 8298 (2009)

R.Nakanishi, et al., Phys. Rev. B 86, 115445 (2012)

Carbon nanotubes can encapsulate various sorts of atomic chains provided that the size of the atom does not exceed the diameter of the nanotube. Cr, Fe, Co, Ni, Cu, Eu, Gd, Cs, Mo, Na, etc.

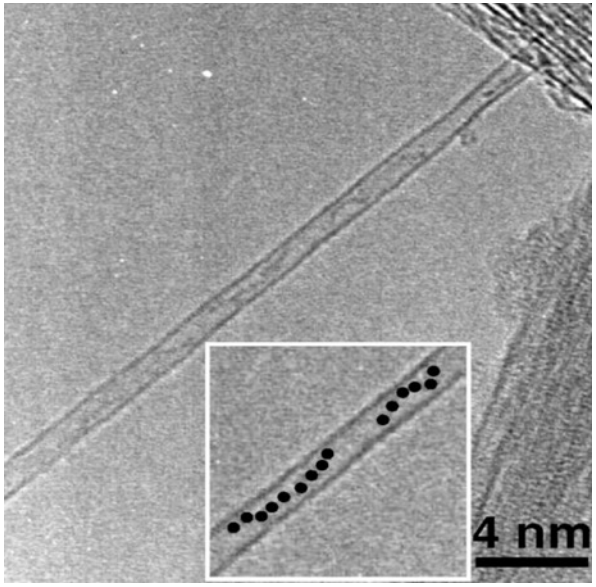

Single-walled CN filled with cesium atoms.

Jeong e.al. PRB68, 075410 (2003)

SEMICONDUCTING CARBON NANOTUBES & METALLIC NANOWIRES (noninteracting)

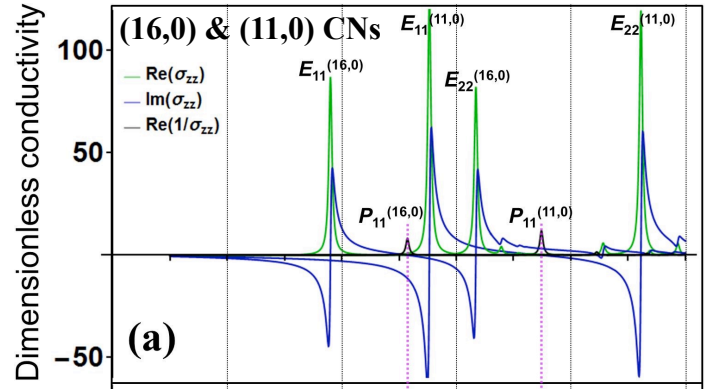

TRANSMISSION BAND
OF THE *FREE* SODIUM ATOMIC WIRE
(100 atoms)

RELATIVE TO
(11,0) *CN*
BANDGAP

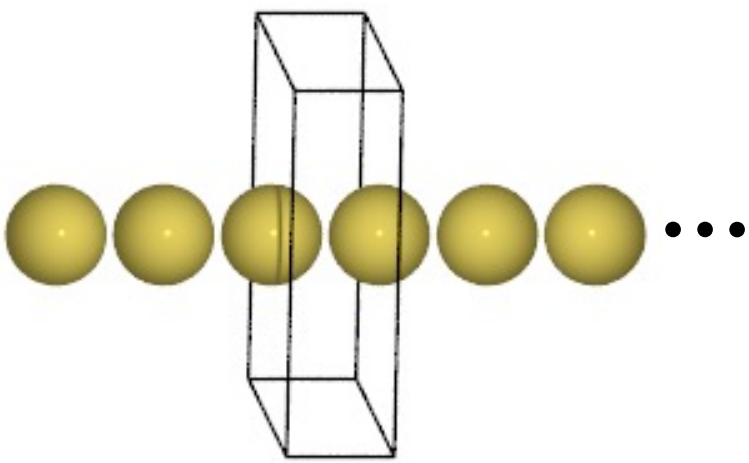

RELATIVE TO
(16,0) *CN*
BANDGAP

HYBRID METAL-SEMICONDUCTOR CARBON NANOTUBE SYSTEM: THE MODEL

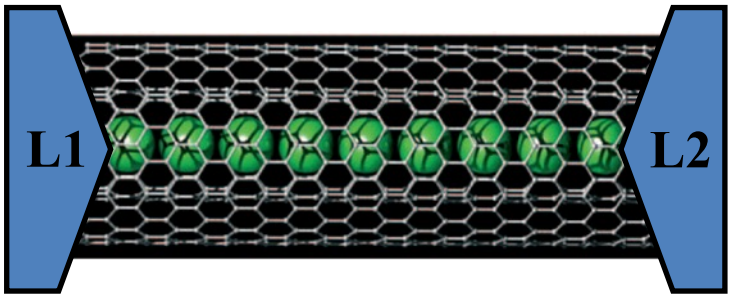

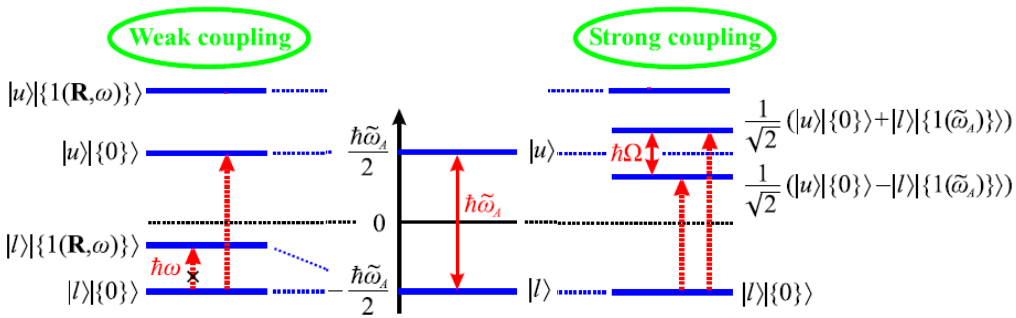

$$T(E) = 4\Delta_1(E)\Delta_N(E)|G_{1N}(E)|^2$$

Mujica, Kemp, & Ratner, J. Chem. Phys. 101, 6849, 6856 (1994)
[Scattering matrix formalism for molecular wires of finite length]

$$\mathbf{G}(E) = [E - \mathbf{H} - \mathbf{\Sigma}(E)]^{-1}, \ \Sigma_{NN}(E) = \Lambda_N - i\Delta_N, \ \Sigma_{11}(E) = \Lambda_1 - i\Delta_1$$

$$\hat{H} = \hat{H}_{\mathrm{AW}} + \hat{H}_{\mathrm{CN}} + \hat{H}_{\mathrm{int}}$$

Gelin & Bondarev, PRB93, 115422 (2016)

$$\hat{H}_{\mathrm{AW}} = E_0 \sum_{k=1}^{N} B_k^\dagger B_k + V \sum_{k=1}^{N-1} (B_k^\dagger B_{k+1} + B_{k+1}^\dagger B_k)$$

$$\hat{H}_{\mathrm{CN}} = \sum_{\mathbf{n}} \int_0^\infty d\omega \hbar\omega \hat{f}^\dagger(\mathbf{n},\omega)\hat{f}(\mathbf{n},\omega) \approx E_p \hat{f}^\dagger \hat{f}$$

$$\hat{H}_{\mathrm{int}} = \sum_{k=1}^{N} \mu_k (B_k \hat{f}^\dagger + B_k^\dagger \hat{f}), \ \mu_k = \mu \lesssim \hbar g = \sqrt{\frac{2\pi d_z^2 \hbar\tilde{\omega}_A}{\tilde{V}}} \approx \sqrt{\frac{2\alpha^3}{\pi}} \frac{\hbar c}{R_{\mathrm{CN}}}$$

Bondarev, Optics Express 23, 3971 (2015) [and Refs. therein]

$$\{B_k^\dagger|0\rangle\}_{k=1,\ldots,N}, \hat{f}^\dagger|0\rangle$$

$$\mathbf{H} = \begin{bmatrix} E_0 & V & 0 & \ldots & 0 & 0 & \mu \\ V & E_0 & V & \ldots & 0 & 0 & \mu \\ 0 & V & E_0 & \ldots & 0 & 0 & \mu \\ \vdots & \vdots & \vdots & \ddots & \vdots & \vdots & \vdots \\ 0 & 0 & 0 & \ldots & E_0 & V & \mu \\ 0 & 0 & 0 & \ldots & V & E_0 & \mu \\ \mu & \mu & \mu & \ldots & \mu & \mu & E_p \end{bmatrix} \quad N+1$$

$$\longleftarrow \quad N+1 \quad \longrightarrow$$

TRANSMISSION VERSUS ENERGY AND WIRE-CN COUPLING

sodium wire of N=10 atoms long; wire-lead coupling Δ = 0.05 eV

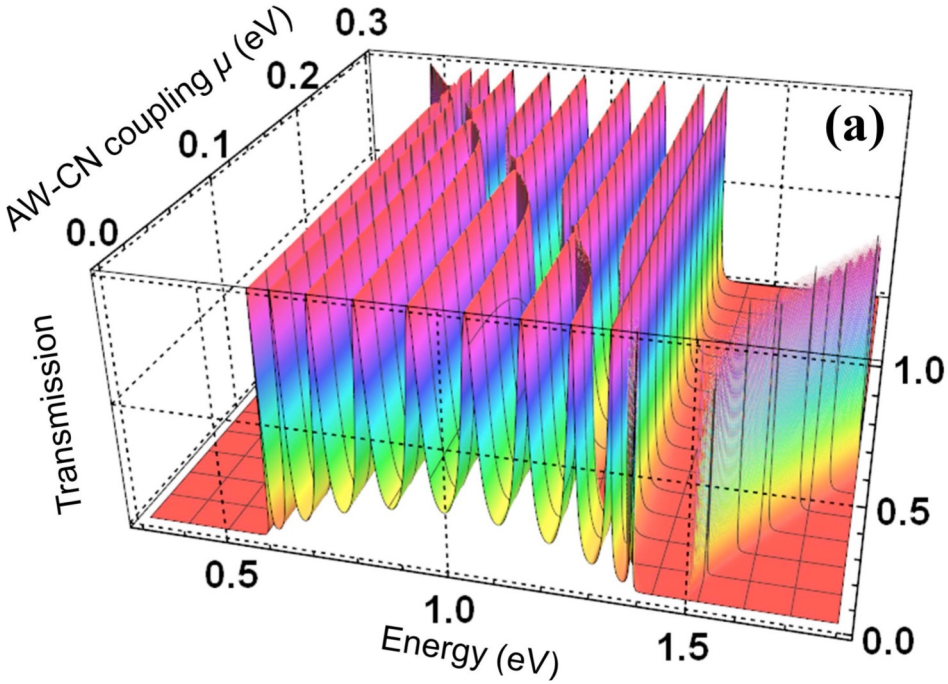

(11,0) CN

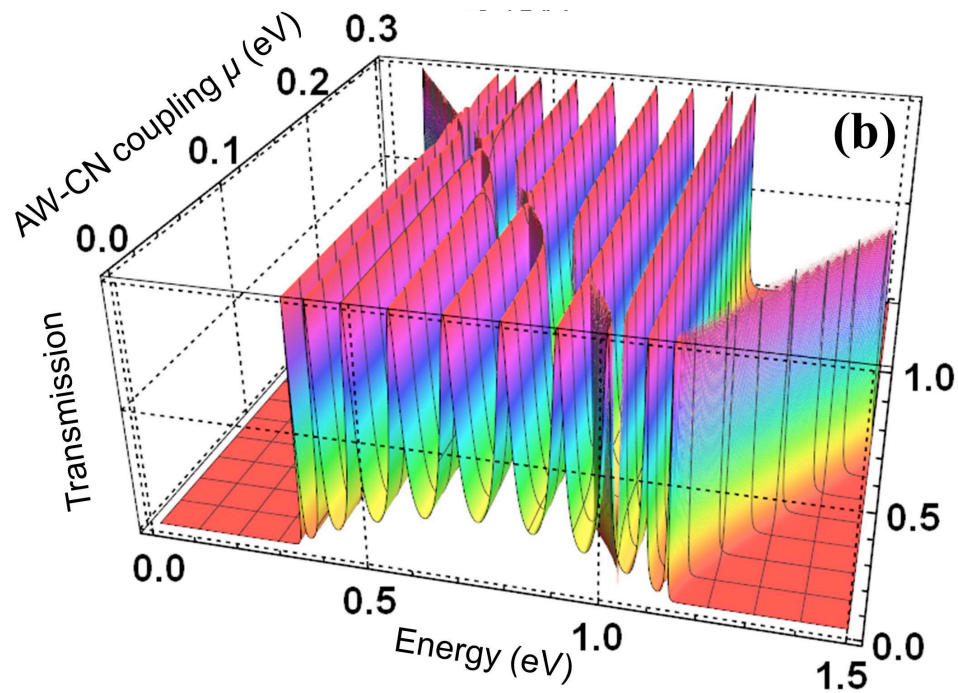

(16,0) CN

$$(E_p - E)(E_0 - E + 2V) = N\mu^2$$

$$E_{1,2} = \tfrac{1}{2}[E_0 + 2V + E_p \pm \sqrt{(E_0 + 2V - E_p)^2 + 4N\mu^2}]$$

Gelin & Bondarev, PRB93, 115422 (2016)

TRANSMISSION VERSUS ENERGY

sodium wire of N=100-103 atoms

μ = 0.045 eV, Δ = 0.1 eV

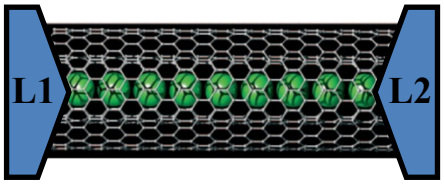

TRANSMISSION VERSUS WIRE LENGTH AT $E=E_0=E_F$

sodium wire inside (11,0) CN

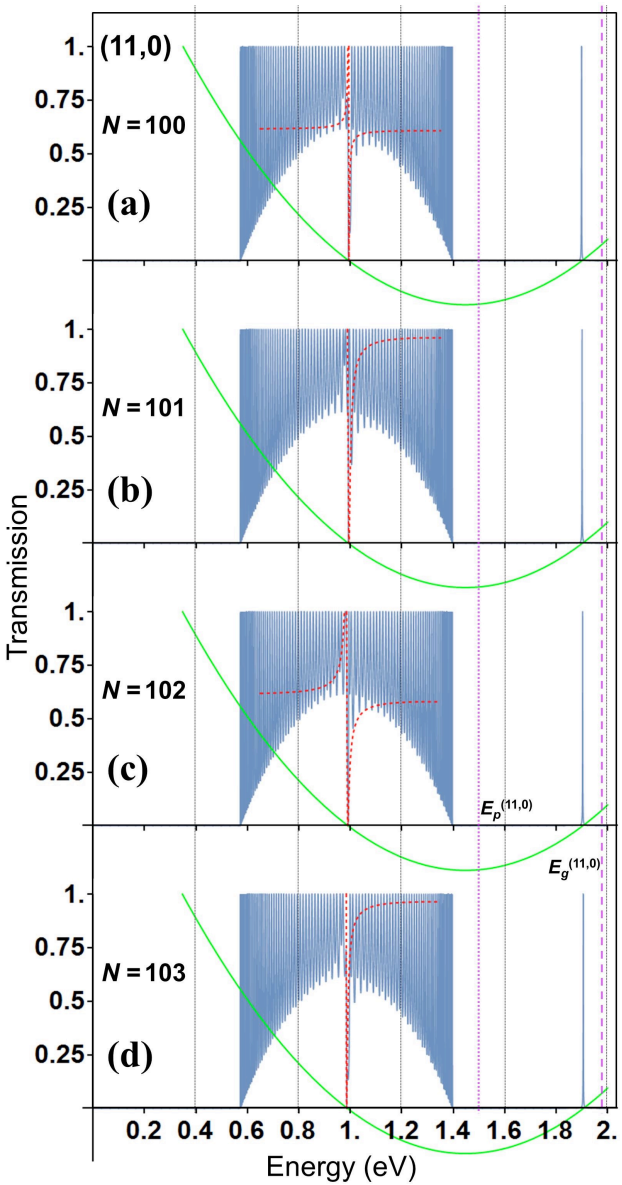

$$(E_p - E)(E_0 - E + 2V) = N\mu^2$$

$$\Gamma \approx \frac{\mu^2 \kappa(\xi, N)}{|E_0 - 2V - E_p|}, \quad \xi = \Delta / V$$

$$2V(E_p - E_F) = N\mu^2$$

N *– number of atoms on the wire*
V *– wire electron hopping constant*
μ *– near-field coupling of electrons on the wire to a CN plasmon mode*
Δ *– wire coupling to the leads*
Γ – Fano resonance width

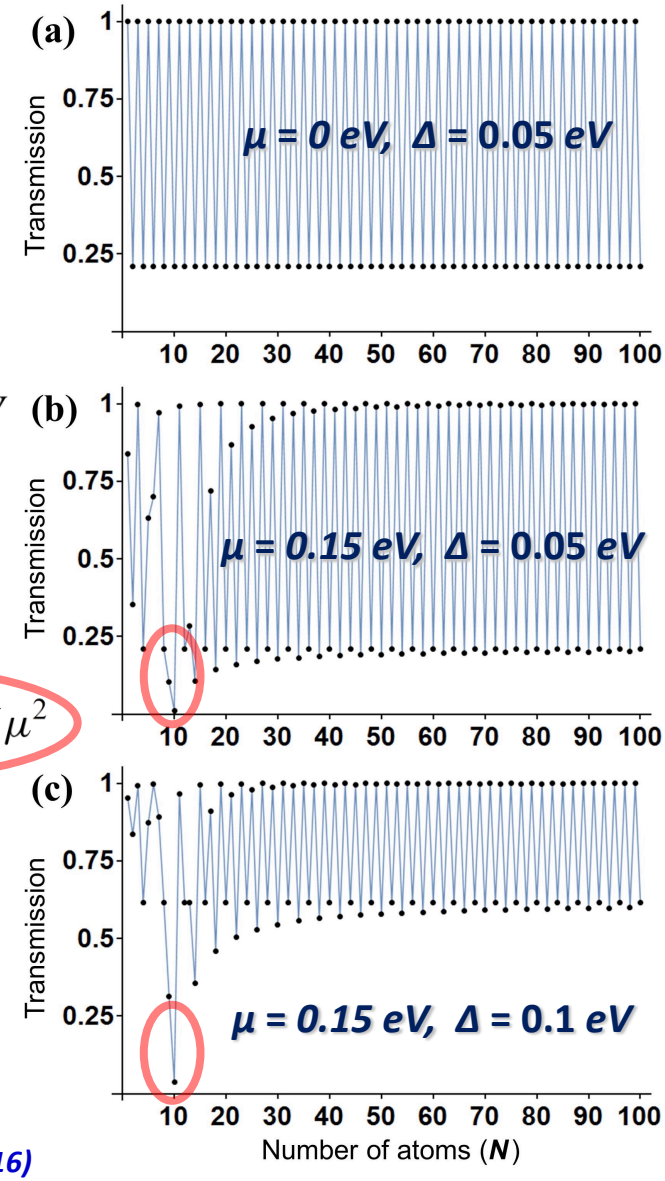

Gelin & Bondarev, PRB93, 115422 (2016)

ULTRATHIN SWCN ARRAYS

Anisotropic Collective Optical Response

I.V. Bondarev and C.M. Adhikari, Physical Review Applied 15, 034001 (2021)

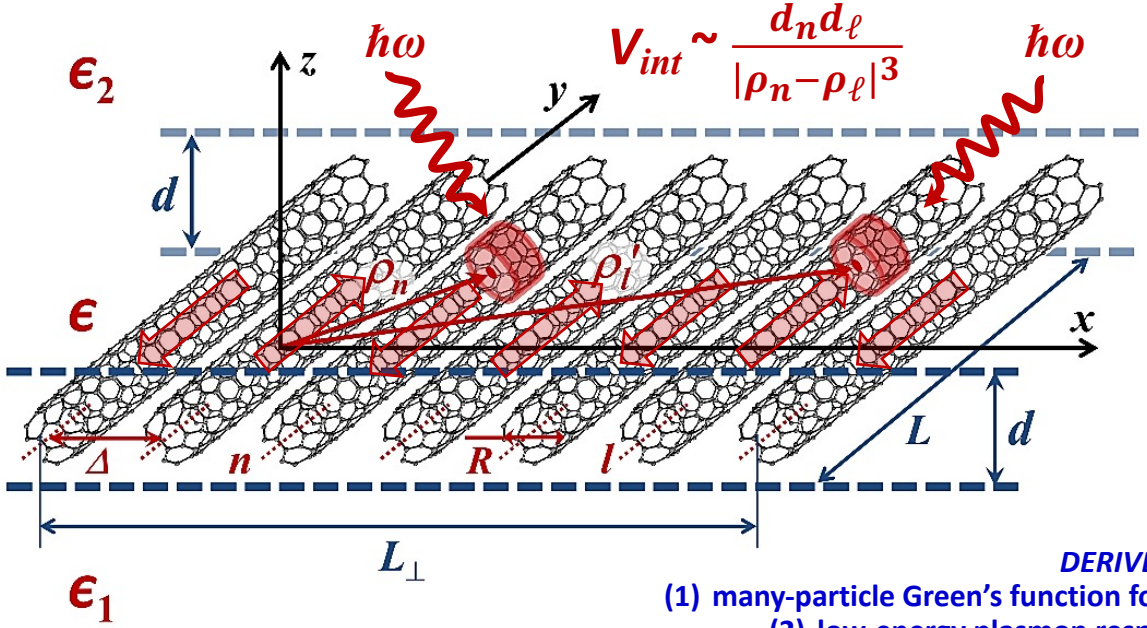

SWCNs cross-talk to each other through the exciton dipole-dipole coupling

DERIVED using:

(1) many-particle Green's function formalism in Matsubara formulation

(2) low-energy plasmon response calculation technique

$$\frac{\varepsilon_{yy}(q,\omega)}{\epsilon} = 1 - \frac{2 f_{\rm CN}\, \sigma_{yy}(q,\omega)}{f_{\rm CN}\, \sigma_{yy}(q,\omega) + i\omega e^2 N_{2\rm D} R/m^* \omega_p^2(q) d}$$

σ_{yy} is the isolated CN longitudinal conductivity

$$\omega_p(q) = \omega_p^{3D} \sqrt{\frac{2qRI_0(qR)K_0(qR)}{1 + (\varepsilon_1 + \varepsilon_2)/\varepsilon q d}}$$

$\omega_p^{3D} = \sqrt{4\pi e^2 N_{3D}/\varepsilon m^*}$ is the *effective* bulk plasma frequency ($N_{3D} = N_{2D}/d$ being the *volumetric* electron density)

$$\varepsilon_{xx}(q,\omega) = \epsilon,$$

$f_{\rm CN}$ is the SWCN volume fraction in the dielectric layer

(1) G. D. Mahan, Many-particle physics, NY 2000

(2) I.V.Bondarev, Opt. Mater. Express 9, 285 (2019)

ULTRATHIN SWCN ARRAYS

General Properties of Collective Excitations

I.V. Bondarev and C.M. Adhikari, Physical Review Applied 15, 034001 (2021)

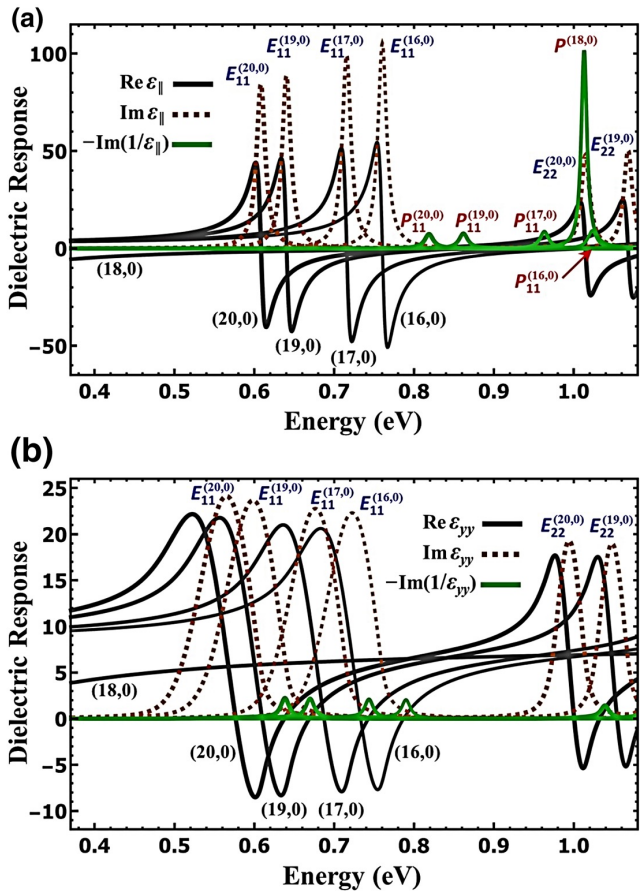

FIG. 4. (a) Individual dielectric responses along the CN axis (longitudinal) for the zigzag (16,0), (17,0), (18,0), (19,0), and (20,0) SWCNs *in vacuum*, obtained using the $\mathbf{k}\cdot\mathbf{p}$ method of the SWCN band-structure calculations [28]. All graphs are scaled down vertically by a factor of 10 for better visibility. (b) Respective room-temperature dielectric response functions along the CN alignment direction, calculated for $d = \Delta = 2R$.

$$\hbar\omega_s(q) = \sqrt{E_s^2(q) + 2E_s(q)V_{ss}(q)}$$

V_{int}

s =1,2,… – 1st, 2nd exciton resonance of an individual SWCN

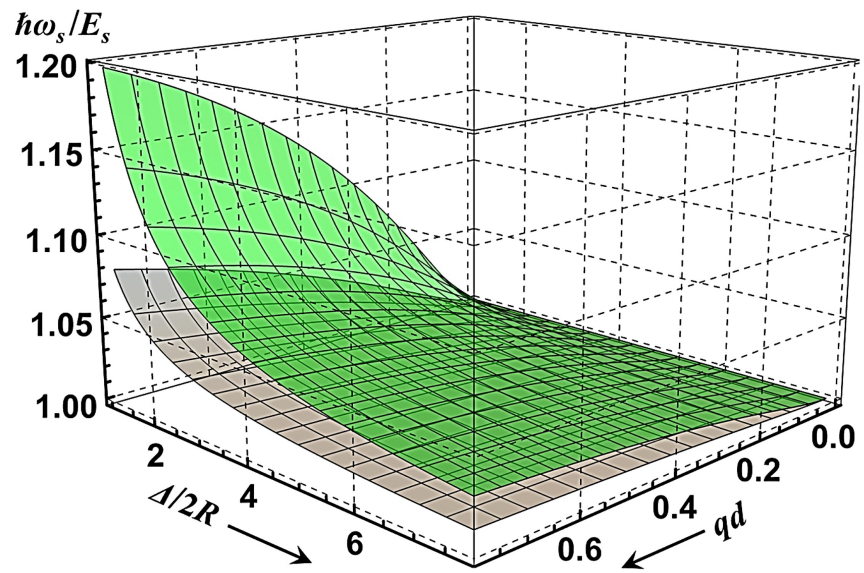

FIG. 2. Dispersion of collective excitations in the ultrathin SWCN arrays with $R/d = 0.5$ (green) and 0.25 (gray) relative to the isolated SWCN exciton dispersion as a function of array parameters qd and $\Delta/2R$.

EXPLORING EFFECTS OF ANISOTROPY IN SWCN FILMS

Finite-Thickness Effects in Ultrathin SWCN Plasmonic Films

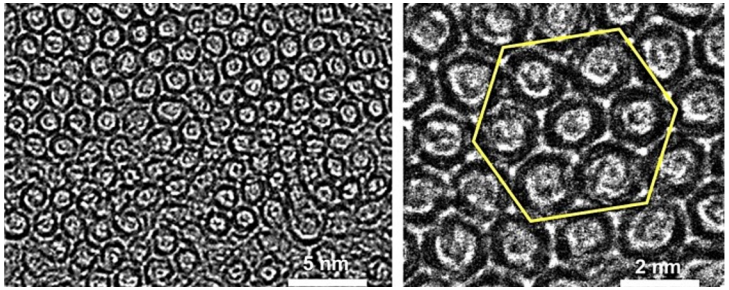

Aligned Carbon Nanotube Films (cross-sectional view): Jun Kono group @ Rice; Abram Falk @ IBM; Jon Fan group @ Stanford; see, e.g., Nano Lett. 19, 3131 (2019)

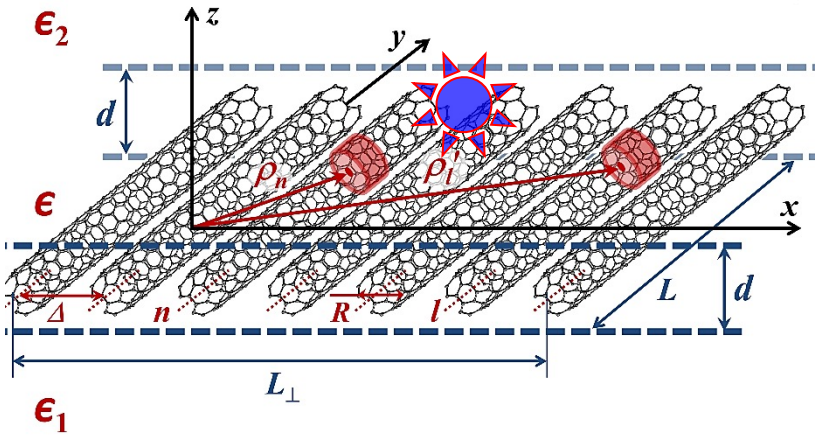

$$\hat{\varepsilon}(q,\omega) = \begin{bmatrix} \varepsilon_{xx} & 0 \\ 0 & \varepsilon_{yy} \end{bmatrix} = \begin{bmatrix} \epsilon & 0 \\ 0 & \varepsilon_{yy}(q,\omega) \end{bmatrix}$$

$$\frac{\varepsilon_{yy}(q,\omega)}{\epsilon} = 1 - \frac{2 f_{\rm CN}\,\sigma_{yy}(q,\omega)}{f_{\rm CN}\,\sigma_{yy}(q,\omega) + i\omega e^2 N_{2\rm D} R/m^* \omega_p^2(q) d}$$

σ_{yy} is the isolated CN longitudinal conductivity

$$\omega_p(q) = \omega_p^{3D}\sqrt{\frac{2qRI_0(qR)K_0(qR)}{1+(\varepsilon_1+\varepsilon_2)/\varepsilon q d}}$$

$\omega_p^{3D} = \sqrt{4\pi e^2 N_{3D}/\varepsilon m^*}$ is the *effective* bulk plasma frequency ($N_{3D} = N_{2D}/d$ being the *volumetric* electron density)

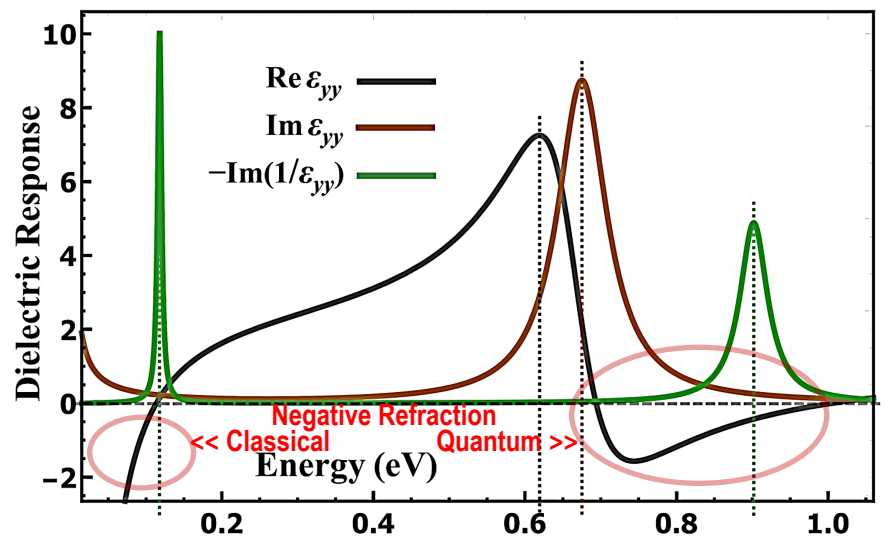

FIG. 5. The room-temperature (300 K) in-plane dielectric response functions along the CN alignment direction calculated for an ultrathin (∼10 nm) weakly inhomogeneous TD film of the MG-mixed (16,0), (17,0), (18,0), (19,0) and (20,0) SWCN

Thickness Controlled

Unidirectional

Spontaneous Emission Enhancement

I.V.Bondarev & C.M.Adhikari, PR Applied 15, 034001 (2021)
I.V.Bondarev, Opt. Mater. Express 9, 285 (2019)

EXCITON-PLASMON COUPLING
in a Designed Mixture of SWCN Arrays

C.M. Adhikari and I.V. Bondarev, Journal of Applied Physics 129, 015301 (2021)

Thermally averaged (300 K) longitudinal dielectric response functions
for the ultrathin ***arrays*** of the (10,0) and (11,0) SWCNs along the CN alignment direction.
Here $d = 3R$ and $\Delta = 3R$ of the respective SWCN

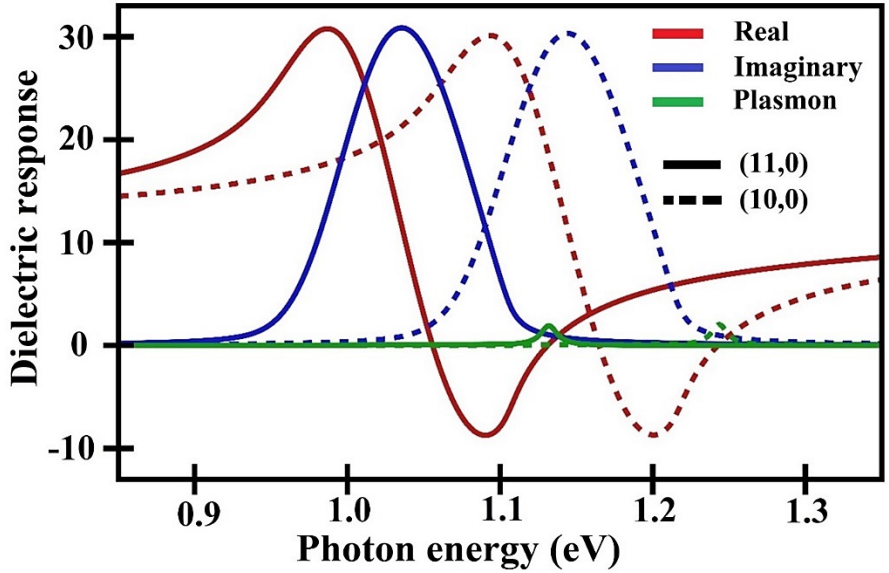

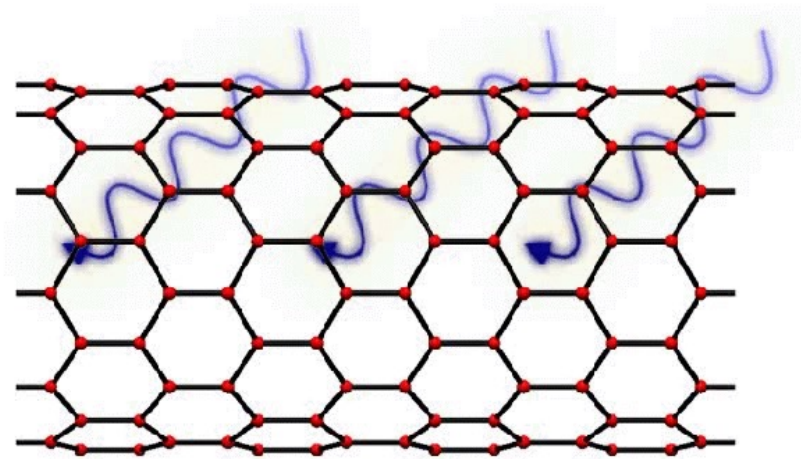

- Due to screening and spatial dispersion, in the *homogeneous* SWCN film the plasmon resonance is positioned much closer in energy to the exciton resonance than it occurs in an individual isolated SWCN

- The plasmon peak of the (11,0) SWCN array is almost exactly in resonance with the exciton absorption peak of the (10,0) SWCN array, to result in a strong exciton-plasmon coupling

- Thermal average:

$$\langle \varepsilon(T,x) \rangle = \sum_q f_s(q,T)\, \varepsilon(T,x), \qquad f_s(q,T) = \frac{1}{Q}\, e^{-\beta\hbar\omega_s}$$

EXCITON-PLASMON COUPLING
in a Designed Mixture of SWCN Arrays

C.M. Adhikari and I.V. Bondarev, Journal of Applied Physics 129, 015301 (2021)

Lineshape profiles of the first exciton absorption resonance

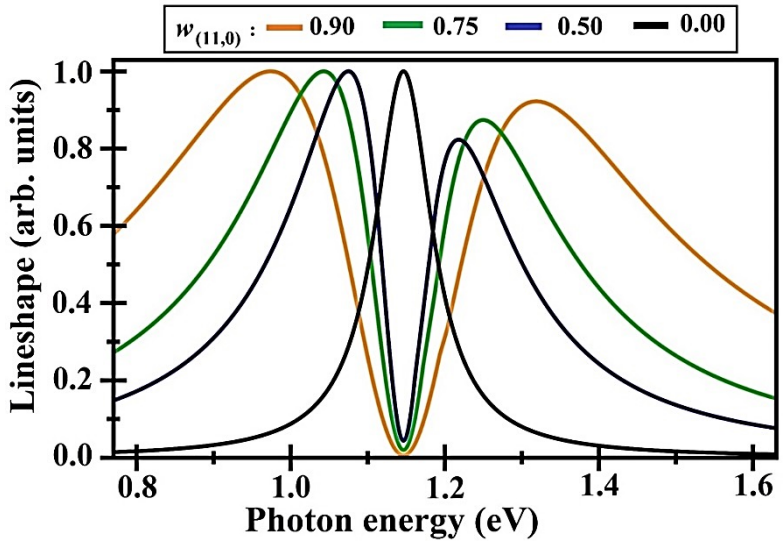

Rabi-splitting as a function of weights of (11,0) CN Array

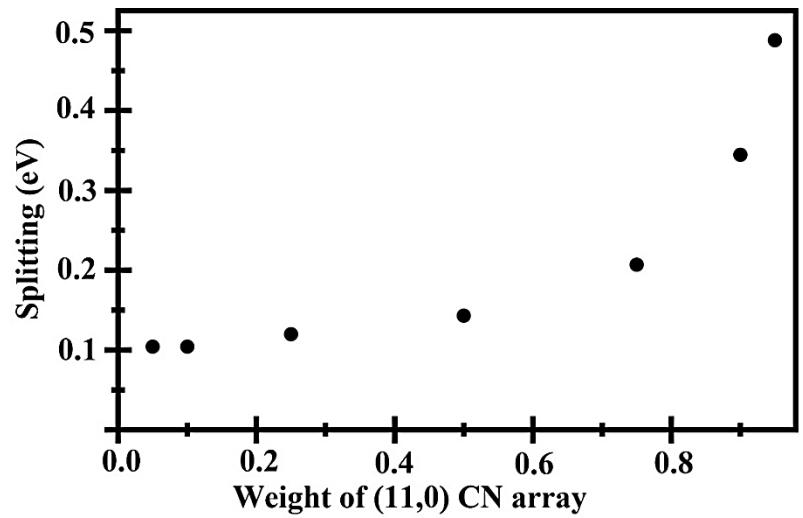

- All profiles exhibit the line-splitting (aka Rabi-splitting), which is a signature of the strong exciton-plasmon coupling
- The larger weight of the (11,0) CN array results in an increased broadening and a greater splitting of entire absorption profile
- The splitting quickly decreases with the reduction of the (11,0) CN array relative weight, to eventually turn into a single-peak resonance absorption profile for zero relative weight of the (11,0) CN array in the mixture
- The larger Rabi-splitting indicates the stronger exciton-plasmon coupling and the decreased light absorption

***Resonance Absorption Lineshape Profile*:**
I.V.Bondarev, Optics Express 23, 3971 (2015)

SUMMARY

- **NANOOPTOPLASMONICS WITH PRISTINE AND HYBRID QUASI-1D SYSTEMS.**
- **Examples outlined and theoretical perspectives:**

(1) Controlled absorption due to plasmon generation by optically excited excitons in individual CNs;

(2) Quasi-1D exciton BEC in individual semiconducting CNs due to the exciton-plasmon coupling controlled by a perpendicular electrostatic field applied *[~1 V/nm, T<100 K experimentally accessible, opens up perspectives to develop coherent polarized light source with CNs]*;

(3) Trions are more stable in strongly confined quasi-1D structures with small reduced *e-h* masses; biexcitons are more stable in less confined structures with large reduced *e-h* masses *[spinoptronics & nonlinear optics in quasi-1D];*

(4) Plasmon enhanced Raman scattering near SWCNs *[single molecule/atom/ion detection, precision spontaneous emission control, optical manipulation];*

(5) Electron transmission Fano resonances in hybrid metal-encapsulating semiconducting CNs;

(6) For a homogeneous 2D array of periodically aligned SWCNs, the real part of the dielectric response function in the alignment direction has NR bands, the film behaves as a 1D hyperbolic metamaterial – <u>adjustable up to optical range;</u>

(7) In a mixture of periodically aligned SWCNs arrays of close diameters, the exciton and plasmon resonances of different arrays are likely to overlap, making the <u>exciton-plasmon coupling</u> possible, which can be used to control optical absorption in the respective frequency domain

PUBLICATIONS:

- I.V.Bondarev & C.M.Adhikari, Physical Review Applied 15, 034001 (2021)
- C.M.Adhikari & I.V.Bondarev, Journal of Applied Physics 129, 015301 (2021)
- I.V.Bondarev, Optical Materials Express 9, 285 (2019)
- I.V.Bondarev & A.Popescu, MRS Advances 2, 2401 (2017)
- I.V.Bondarev, Modern Physics Letters B 30, 1630006 (2016)
- M.F.Gelin & I.V.Bondarev, Physical Review B 93, 115422 (2016)
- I.V.Bondarev, Optics Express 23, 3971 (2015)
- I.V.Bondarev & A.V.Meliksetyan, Physical Review B 89, 045414 (2014)
- I.V.Bondarev, Physical Review B 90, 245430 (2014)
- M.F.Gelin, I.V.Bondarev, and A.Meliksetyan, J. Chem. Phys. 140, 064301 (2014)
- M.F.Gelin, I.V.Bondarev, and A.Meliksetyan, Chem. Phys. 413, 123 (2013)
- L.M.Woods, A.Popescu, D.Drosdoff, & I.V.Bondarev, Chemical Physics 413, 116 (2013)
- I.V.Bondarev, Physical Review B 85, 035448 (2012)
- A.Popescu, L.M.Woods, & I.V.Bondarev, Physical Review B 83, 081406(R) (2011)
- I.V.Bondarev, Physical Review B 83, 153409 (2011)
- I.V.Bondarev, Journal of Computational & Theoretical Nanoscience 7, 1673 (2010)
- I.V.Bondarev, L.M.Woods, & K.Tatur, Physical Review B 80, 085407 (2009)
- I.V.Bondarev and B.Vlahovic, Physical Review B 74, 073401 (2006)
- I.V.Bondarev and Ph.Lambin, Physical Review B 72, 035451 (2005)
- I.V.Bondarev and Ph.Lambin, Physical Review B 70, 035407 (2004)

THANK YOU !!

COLLABORATORS:

USF UNIVERSITY OF SOUTH FLORIDA COLLEGE OF ARTS & SCIENCES

Lilia Woods group

Wolfgang Domcke group